

## REVIEW ARTICLE

# Structural similarities of Na,K-ATPase and SERCA, the Ca<sup>2+</sup>-ATPase of the sarcoplasmic reticulum

Kathleen J. SWEADNER<sup>1</sup> and Claudia DONNET

Neuroscience Center, Massachusetts General Hospital, 149-6118, 149 13th Street, Charlestown, MA 02129, U.S.A.

The crystal structure of SERCA1a (skeletal-muscle sarcoplasmic-reticulum/endoplasmic-reticulum Ca<sup>2+</sup>-ATPase) has recently been determined at 2.6 Å (note 1 Å = 0.1 nm) resolution [Toyoshima, Nakasako, Nomura and Ogawa (2000) *Nature* (London) **405**, 647–655]. Other P-type ATPases are thought to share key features of the ATP hydrolysis site and a central core of transmembrane helices. Outside of these most-conserved segments, structural similarities are less certain, and predicted transmembrane topology differs between subclasses. In the present review the homologous regions of several representative P-type ATPases are aligned with the SERCA sequence and mapped on to the SERCA structure for comparison. Homology between SERCA and the Na,K-ATPase is more extensive than

with any other ATPase, even PMCA, the Ca<sup>2+</sup>-ATPase of plasma membrane. Structural features of the Na,K-ATPase are projected on to the Ca<sup>2+</sup>-ATPase crystal structure to assess the likelihood that they share the same fold. Homology extends through all ten transmembrane spans, and most insertions and deletions are predicted to be at the surface. The locations of specific residues are examined, such as proteolytic cleavage sites, intramolecular cross-linking sites, and the binding sites of certain other proteins. On the whole, the similarity supports a shared fold, with some particular exceptions.

**Key words:** cross-linking, crystal structure, membrane protein, protein folding, P-type ATPases.

## INTRODUCTION

The high-resolution crystal structure of the SERCA1a (skeletal-muscle sarcoplasmic-reticulum/endoplasmic-reticulum Ca<sup>2+</sup>-ATPase) [1] is the first reported structure of an active transport protein. Unlike the elegant symmetry of the K<sup>+</sup> channel [2], this enzyme proved to be a complex protein with distinct domains that are thought to undergo major movements in the course of a single turnover [3]. Within the membrane, a pocket is formed by kinks in transmembrane  $\alpha$ -helices to make an ion-binding site that simultaneously accommodates two Ca<sup>2+</sup> ions. There is considerable evidence from lower-resolution images that two related ATPases, the Na,K-ATPase and the proton ATPase of *Neurospora*, have important structural features in common with SERCA1a [4–8].

The P-type ATPases are enzymes that transport ions or molecules across biological membranes with the energy of hydrolysis of ATP. The designation P-type comes from the mechanism: the terminal phosphate of ATP is transiently transferred to an aspartate residue in the active site, resulting in reversible conformation changes [9,10]. The P-type ATPases fall into five or more classes and subclasses. The type II class of P-type ATPases to which SERCA and the Na,K-ATPase belong shows clear evolutionary relationships that justify a separate grouping from P-type ATPases that transport protons, less abundant metal ions, Mg<sup>2+</sup>, and from the aminophospholipid transferases and other related enzymes [11,12]. Alignments of SERCA with members of other subclasses of the gene family have been performed, however, leaving no doubt about the likelihood that the structures are related [9,12,13].

Extensive work on the structures of certain type II and III ATPases has shown a common theme: there is a catalytic subunit

of about 100 kDa with usually ten predicted transmembrane spans and four intracellular loops that differ greatly in length. A large fraction of the mass of the protein is found in the L4–5 intracellular loop, which has long been known to be the location of the ATP and phosphorylation sites (transmembrane spans are numbered M1, etc.; extramembranous loops are identified by the flanking membrane spans; i.e. L4–5 is the loop between spans M4 and M5). Critical residues of the ATP-binding site map some distance away from the covalent phosphorylation site at D\*KTGT (where D\* represents the aspartate residue that is phosphorylated), leading to the inference that there are ATP-binding and phosphorylation domains that come together in the course of the enzyme reaction cycle. These conformation changes are thought to influence the structure of the transmembrane domain, where ion-binding sites must reside, by altering the tilt or depth of critical membrane segments in much the same way that the handles of scissors control the blades [10]. There has been considerable controversy, however, about the extent of similarity of the membrane topology of the Ca<sup>2+</sup>-ATPase of sarcoplasmic reticulum and even closely related ATPases like the Na,K-ATPase in the C-terminal third of the protein [9,14].

## ANALYTICAL METHODS

Cn3D 3.0, a program available in the structure division of the National Center for Biotechnology Information (NCBI; website <http://www.ncbi.nlm.nih.gov>), displays crystal structures in a rotatable format that permits many user-specified features. It also permits the import of the amino acid sequences of related proteins for comparison. With two or more sequences, it performs a gapped-BLAST alignment using the associated linear alignment utility, DDV (an abbreviation from the French for two-

Abbreviations used: SERCA, sarcoplasmic-reticulum/endoplasmic-reticulum Ca<sup>2+</sup>-ATPase; SERCA1a, skeletal-muscle SERCA; PMCA, plasma-membrane Ca<sup>2+</sup>-ATPase; NCBI, National Center for Biotechnology Information; BIPM, *N*-[*p*-(2-benzimidazolyl)phenyl]maleimide; SDSM, 4-acetamidomaleimidylstilbene-2,2'-disulphonic acid; C<sub>12</sub>E<sub>10</sub>, deca(ethylene glycol) monododecyl ether; A domain, activation domain; P domain, phosphorylation domain; N domain, nucleotide-binding domain.

<sup>1</sup> To whom correspondence should be addressed (e-mail [sweadner@helix.mgh.harvard.edu](mailto:sweadner@helix.mgh.harvard.edu)).

dimensional viewer), and displays the similarities both in linear format and with several colour-coded options for visualization on the original crystal structure. All of the structure Figures shown in this review were prepared with the same program, employing different specific formatting styles depending on the application. Cn3D is not a modelling program that can predict a new hypothetical structure, but it does allow one to show on one structure (SERCA1a) the extent of sequence alignment with a second protein, and the predicted locations of the other proteins' features.

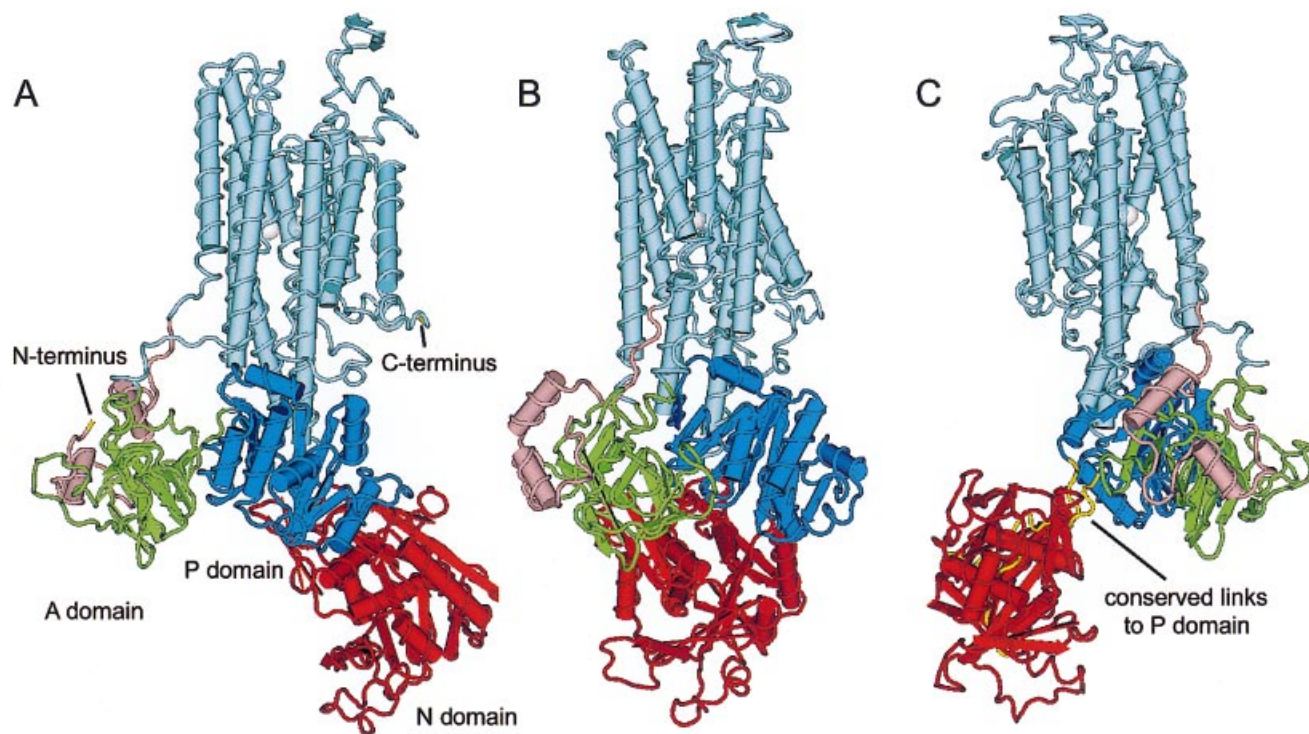
Gapped-BLAST [15] is the most commonly used algorithm for alignment of sequences, and for protein sequences the program utilizes a matrix of amino-acid-substitution probabilities (BLOSUM62) that takes into account the underlying genetic code. The structure files used for SERCA1a were MMDb (Molecular Modeling DataBase) Id 13684 and PDB (Protein DataBase) Id 1EUL. The Na,K-ATPase rat  $\alpha 1$  sequence aligned with it was from GenBank® (accession no. M14511); other sequences used are listed in Table 1 below.

### PRINCIPAL FEATURES OF SERCA1a

The 2.6 Å crystal structure of SERCA1a has provided a structural basis for the prevailing model of ATPase mechanism that is

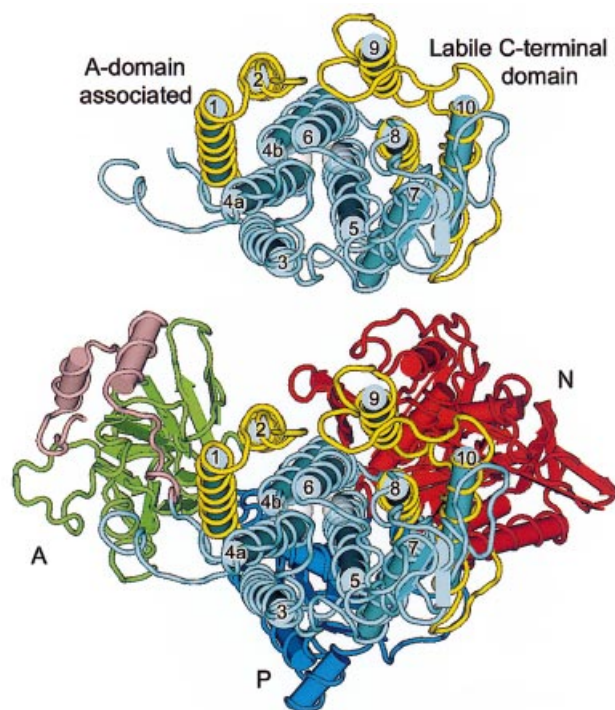
consistent with much of the prior literature ([1] and the accompanying Review [16]). The most notable feature of the structure is the segregation of the  $\alpha$  subunit mass into four separate domains. Figure 1 shows several views of the crystal structure to illustrate its domains and their terminology. The Figure employs the Cn3D 'secondary structure' display format, in which  $\alpha$ -helices appear as cylinders and  $\beta$ -strands as arrows, and a thread follows the C $\alpha$  backbone. The 'domain' colouring scheme gives each domain a different colour. Because the program does not represent depth very well, several rotations are shown. In Figures 1(A) and 1(C) the relative isolation of the A ('actuator', green and pink) and N (nucleotide-binding, red) domains can be seen. The highly conserved P (phosphorylation) domain is anchored to the membrane domain. A useful simplified diagram can be found in a commentary by MacLennan and Green [17].

Figure 2 shows the arrangement of  $\alpha$ -helices in the membrane domain. In the upper panel, the spans are shown from the luminal side of the membrane with the other portions of the protein cut away, whereas, in the lower panel, the positions of the other domains can be seen below in the cytoplasm. The residues that contribute to Ca<sup>2+</sup> binding are all in M4, M5, M6, and M8. M4 is interrupted by a disruption of helical structure, and so it is shown as M4a and M4b. M6 is also interrupted, and the program does not show the cytoplasmic half as  $\alpha$ -helix.



**Figure 1** Three rotations of the SERCA1a crystal structure

Starting from the N-terminus, the A domain is comprised of the cytoplasmic N-terminus (pink), which forms two short  $\alpha$ -helices, and the first cytoplasmic loop between M1 and M2 (green), which is folded as a distorted jelly-roll structure. This domain is connected to M1, M2, and M3 by long extended sequences that apparently provide conformational flexibility, as the domain is thought to undergo substantial rotation in different conformational states [3]. The transmembrane domain (light blue) contains 10  $\alpha$ -helices of different lengths contributed by both the N-terminal third and the C-terminal third of the molecule. Two co-crystallized Ca<sup>2+</sup> ions appear as white spheres. The large intracellular loop between M4 and M5 is actually folded into two separate domains, one emerging from the other. The portions closest to M4 and M5 come together to form the P domain (blue), with a Rossmann fold including  $\beta$ -sheet contributed by both portions. Extending from this domain is the N domain (red), with a 7-stranded  $\beta$ -sheet sandwiched by helix bundles. This domain is predicted to be hinged to permit it to tilt 20° closer to the P domain, bringing the two halves of the active site together [1]. In (C), yellow highlighting has been used to illustrate the buried location of the conserved segments that link the N domain to the P domain (more below).



**Figure 2** Membrane spans as seen from the outside

The  $\alpha$ -helices comprising the membrane domain are packed at a variety of angles. Two helices, M4 and M6, are interrupted by major kinks, and in fact the first half of M6 is shown by the program as a coil without a cylinder. The transmembrane domain may really constitute two or three folding domains that alter their relationship to one another during active transport. M1 and M2 arguably are dominated by their long attachments to the A domain, and are highlighted in yellow at the left. The C-terminal region appears to form a compact structure consisting of transmembrane spans M7–M10 and associated loops, and this is protease-resistant [65]. Toyoshima et al. describe "... a clear segregation between M1–M6 and M7–M10, consistent with the lack of M7–M10 in bacterial type I P-type ATPases ..." [1]. M8–M10 in Na,K-ATPase show an unusual thermal lability and are highlighted with yellow on the right [42,82,83].

Portions of some of the transmembrane  $\alpha$ -helices (notably M2, M3, M4b and M5) extend into the cytoplasm. Possible subdomains are highlighted with yellow.

#### EXTENT OF SIMILARITY BETWEEN SERCA AND OTHER ATPases

The type II class of P-type ATPases includes all of the enzymes that transport the abundant ions of basic cellular metabolism:  $\text{Ca}^{2+}$ ,  $\text{Na}^{+}$ ,  $\text{K}^{+}$  and  $\text{H}^{+}$  exchanged for  $\text{K}^{+}$  [9,11,18–20]. Type I ATPases include those that transport heavy metals, and also ATPases of bacteria that require additional subunits. The type III ATPases include the proton pumps of fungi and the  $\text{Mg}^{2+}$ -ATPases of bacteria. The type IV ATPases include more distantly related proteins, most of which have still-undefined functions. Members of this group are implicated in the transport of hydrophobic substances, such as aminophospholipids [20], and mutation in one blocks enterohepatic bile-salt circulation [21]. Axelsen and Palmgren's paper [12] contains an extensive list that includes a group termed 'type V' and additional unclassified sequences (see also [20] and the website <http://www.biobase.dk/~axe/Patbase.html>). Most of the subgroups are represented in all three domains of life (eukaryotic, bacterial and archaeal). That there are sequence similarities among members of the P-ATPase family is well known [9,18], but it is informative to visualize their alignment with the  $\text{Ca}^{2+}$ -

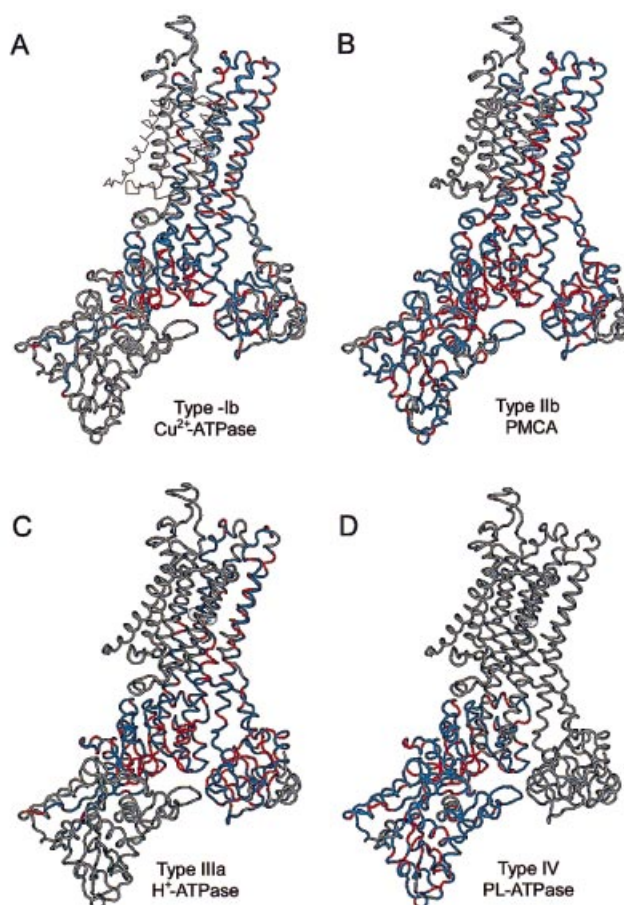


**Figure 3** Patterns of similarity between SERCA and other classes of P-type ATPases

Gapped-BLAST alignments of SERCA structure with the sequences of representatives of four other groups of P-type ATPases. The N, P, A and membrane domains correspond to those in Figure 1(A), but seen from the other side. Red represents identical residues, blue represents residues that are conserved and/or aligned, and grey is sequence that does not align with anything in the paired sequence. Although all classes are homologous in the P domain, the extent of similarity in the other domains varies between classes. It is notable that the other class of  $\text{Ca}^{2+}$ -ATPase, PMCA, lacks alignment in the last four membrane spans.

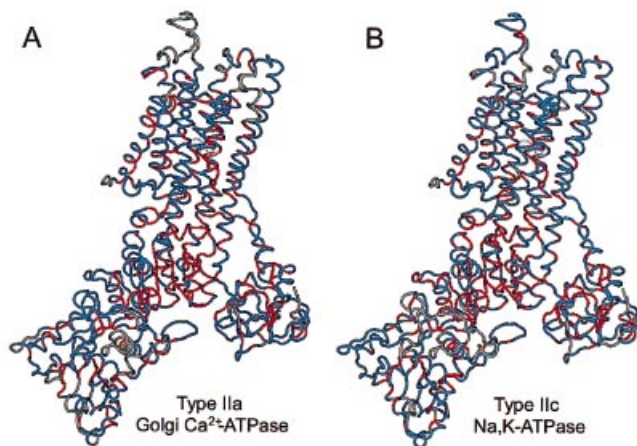
ATPase by mapping homologous regions on to its structure. This was done by using gapped-BLAST to align each family member with the SERCA sequence in Cn3D. Figure 3 shows four representative examples of P-type ATPases of different classes. SERCA1a itself is in the IIa group, and the Figure shows examples of alignable regions from group Ib [human  $\text{Cu}^{2+}$ -ATPase (Wilson's disease)], group IIb (human plasma-membrane  $\text{Ca}^{2+}$ -ATPase, PMCA1b), group IIIa ( $\text{H}^{+}$  ATPase of *Neurospora crassa*) and group IV (a putative aminophospholipid translocase of *Saccharomyces cerevisiae*). The SERCA structure is shown in 'worm' format, in which the  $\alpha$ -carbon backbone is traced smoothly. The colours are in the 'conservation' format: red represents identical residues, blue represents other homologous and aligned residues, and grey represents SERCA sequence that shows no alignment with the paired protein as detected with gapped-BLAST. Portions of each paired ATPase that have no correspondence with SERCA are, of course, not visible at all.

Of these four examples, the PMCA (Figure 3B) has the most extensive homology with SERCA. All of the phosphorylation (P)

**Table 1** Gapped BLAST alignment patterns for representatives of the four major classes of P-type ATPases

This Table shows some features of the alignment of SERCA 1a (rabbit muscle) with different P-ATPases. Pair-wise alignments with SERCA revealed relationships that were not obvious in previous evolutionary analyses that were based on P-domain and A-domain regions alone. Groups Ila and Iic (SERCA and Na,K-ATPase) are more closely related to one another than to group Iib (PMCA). The pink shading indicates sequences illustrated in Figures 3 and 4. Key to symbols: empty space, no alignment at all; + + +, alignment is about 100%; + +, about 80–90%; +, about 50–70%; pc, only connectors to P-domain can be aligned; ■, aligns all amino acids or all but one; ▲, aligns about 70–90% of the segment; □, aligns about half of the segment; NA, no amino acids to align. Genera not already defined: *E.*, *Escherichia*; *M.*, *Mycobacillus*; *S.*, *Salmonella*; *H.*, *Homo*.

Type	Name	Accession number	P domain	A domain	N domain	Membrane domains										
						M1	M2	M3	M4a	M4b	M5	M6	M7	M8	M9	M10
Ia	K <sup>+</sup> -ATPase kdpB ( <i>E. coli</i> )	P03960	+ +	+	p.c.	□	▲	■	■	■	■			NA	NA	NA
	Probable K <sup>+</sup> -ATPase ( <i>M. tuberculosis</i> )	Z92539	+ +	+ +	p.c.	▲	■	▲	▲	■	■			NA	NA	NA
Ib	Cu <sup>2+</sup> -ATPase Wilson ( <i>H. sapiens</i> )	P35670	+ +	+	p.c.	□	▲	▲	■	■	■			NA	NA	NA
	Cu <sup>2+</sup> -ATPase PCA1 ( <i>S. cerevisiae</i> )	P38360	+ +	+	p.c.	▲	▲	■	■	▲	□		NA	NA	NA	NA
Ila	SERCA ( <i>H. sapiens</i> )	P16614	+ + +	+ + +	+ + +	■	■	■	■	■	■	■	■	■	■	■
	Golgi Ca <sup>2+</sup> -ATPase ( <i>S. cerevisiae</i> )	P13586	+ + +	+ +	+ +	■	■	■	▲	■	■	■	■	■	■	■
Iib	PMCA 1b ( <i>H. sapiens</i> )	P20020	+ + +	+	+ +	■	■	■	■	■	■	■	■	■	■	■
	Vacuolar Ca <sup>2+</sup> -ATPase ( <i>S. cerevisiae</i> )	P38929	+ + +	+ +	+ +	■	■	▲	▲	■	■	■	■	■	■	■
Iic	Na <sup>+</sup> ,K <sup>+</sup> -ATPase α1 chain ( <i>H. sapiens</i> )	P05023	+ + +	+ +	+ +	▲	■	■	▲	■	■	■	▲	▲	■	■
	Gastric H <sup>+</sup> /K <sup>+</sup> -ATPase α-chain ( <i>H. sapiens</i> )	P20648	+ + +	+ +	+ +	■	▲	■	▲	■	■	■	▲	■	■	■
Iid	Na <sup>+</sup> -ATPase 1 ( <i>S. cerevisiae</i> )	P13587	+ + +	+ + +	+ +	■	■	■	▲	■	■	■	■	■	■	■
	Na <sup>+</sup> -ATPase 2 ( <i>S. cerevisiae</i> )	Q01896	+ + +	+ + +	+ + +	■	■	■	▲	■	■	■	■	■	■	■
IIIa	H <sup>+</sup> -ATPase PMA1 ( <i>S. cerevisiae</i> )	P05030	+ + +	+ +	p.c.	▲	■	■	■	■	▲	■	■	■	■	■
	H <sup>+</sup> -ATPase ( <i>N. crassa</i> )	P07038	+ + +	+	p.c.	▲	▲	■	▲	■	▲	■	■	■	■	■
IIIb	Mg <sup>2+</sup> -ATPase ( <i>E. coli</i> )	P39168	+ +		+ +						■	■	▲			NA
	Mg <sup>2+</sup> -ATPase ( <i>S. typhimurium</i> )	P22036	+ +	+ + +	+	■	■	■	▲	■	■	■	□	NA	NA	NA
IV	Putative PL-ATPase ( <i>S. cerevisiae</i> )	P39524	+ +		+ +											
	ATPase ( <i>S. cerevisiae</i> )	P40527	+ + +	+	+ +	■	▲	▲	■	■	▲					NA

**Figure 4** Patterns of similarity between SERCA, a yeast homologue, and Na,K-ATPase

Gapped-BLAST alignments of a close yeast relative of SERCA (A) and of Na,K-ATPase (B). Compared with Figure 3 it can be seen that Na,K-ATPase aligns as well as the yeast Ca<sup>2+</sup>-ATPase, and better than PMCA. This was not predicted by studies based on hydropathy plots.

domain and most of the nucleotide-binding (N) domain align, as does the portion of the activation (A) domain from the L2–3 loop (green in Figure 1). The N-terminal portion of the A domain (pink in Figure 1) that comprises the elongated link to the membrane domain is also conserved, along with the second of its two α-helices. In the membrane domain, however, only M1–M6 align with the SERCA ATPase. The program detects no

homology in either the membrane spans or the connecting loops after M6, and attempts to find similarity manually were also unsuccessful. These two different mammalian Ca<sup>2+</sup>-ATPases, then, have a somewhat surprising structural divergence in the C-terminal third, even though four membrane spans are predicted there for PMCA. The PMCA also has additional C-terminal sequence that bears regulatory elements following the last of its predicted transmembrane spans [22,23].

The Wilson's-disease Cu<sup>2+</sup>-ATPase, a type Ib ATPase (Figure 3A) has a longer N-terminus with additional predicted transmembrane spans, and lacks anything corresponding to M8–M10; the latter are consequently shown as thin lines in the Figure. M1–M5 aligned, according to gapped-BLAST, but no homology was detected in M6 or M7. Despite alignment with M1, there was no alignment to the N-terminal portion of the A domain, although the L2–3 portion of the A domain aligned reasonably well. Most of the P domain aligned, but of the N domain, only the two extended stretches that link the N domain to the P domain aligned. The proton pump of *Neurospora* (Figure 3C), for which an 8 Å structure is known [5], is from the type IIIa subclass, but has a pattern of similarity that is rather similar to that of the Cu<sup>2+</sup>-ATPase, although it lacks the additional N-terminal spans and has ten spans like SERCA. Transmembrane spans M1–M5 were aligned to a similar extent, but there was no alignment detected for spans M6–M10, although the available electron-crystallography structure indicates the same number of spans and a similar arrangement. The L2–3 portion of the A domain aligned, as did the extended link to the N-terminus up to and including the second A domain α-helix. As with PMCA (discussed below), however, the first N-terminal α-helix did not align. Like the Cu<sup>2+</sup>-ATPase, very little of the N-domain aligned other than the segments that connect it to the P domain (called 'PC', for P-domain connectors, in Table 1 above).

Figure 3(D) shows the alignment for one of the most distantly related members of the P-type ATPase family, an enzyme that may be an aminophospholipid translocase that maintains the asymmetry of the lipid composition of the membrane [24] (see, however, [25]). Intriguingly, besides the P domain that is conserved in all the family members, it has excellent alignment with the SERCA N-domain, unlike the  $\text{Cu}^{2+}$ -ATPase and *Neurospora* enzymes. For the rest of the protein, however, gapped-BLAST did not detect homology at all. Other members of the type IV group showed better alignment (not shown), so this represents an extreme case.

Table 1 summarizes the gapped-BLAST alignments of a sampling of P-type ATPases with the SERCA structure. Each of the sequences was inspected in the same way as in the examples in Figure 3. The symbols represent the extent of alignment: complete, largely complete and partial. Where a space in the Table is blank, gapped-BLAST did not detect any homology. Strictly speaking, this means that if there is any homology, it fell below the threshold set by the program. Because the substitution probability matrix used was BLOSUM62, it should be borne in mind that a different probability matrix might produce a more sensitive result. With this caveat, some conclusions can be drawn. First, the P domain, with its Rossmann fold comprised of two different portions of the large intracellular loop, is the only consistently conserved segment for the whole gene family. The only portions of the N domain that are always aligned are the extended strands that emerge directly from the two halves of the P domain, the P domain connectors (yellow in Figure 1C). Otherwise, there is little alignment of the N domain for any of the type Ia or Ib ATPases, and excellent alignment with all of type II. It aligned with only one of eight type III sequences examined, and some of type IV. Alignment with the A domain also varies: excellent to reasonably good with types I, II and IIIa, and quite variable with types IIIb and IV. For the transmembrane spans of the SERCA enzyme, no single segment is invariably aligned with other ATPases, but the tendency for maximum alignment with spans M2, M3, M4b and M5 is apparent. M4b and M5 are the helices that connect to the Rossmann fold of the P domain, and all of these most-conserved spans have stalk segments in the cytoplasm.

The classification of subtypes developed by Palmgren and associates [12] was based on eight stretches of core sequence found in all P-type ATPases, not on the full-length sequences, which were too divergent to be aligned in their entirety. It can now be seen that the eight core stretches are not representative of all of the folding domains of the SERCA1a structure: the first three are all in the L2–3 loop portion of the A domain, the fourth is M4, and the rest are all from the P domain, plus one of the connecting links between the P and N domains. The pair-wise gapped-BLAST alignments that we have examined here suggest that groupings based on N domain and membrane domain differences may contribute to further classification of evolutionary relationships between groups.

Figure 4 features the Golgi  $\text{Ca}^{2+}$ -ATPase of yeast (group IIa, like SERCA) and the Na,K-ATPase (group IIc), because they show much more extensive alignment. The sequence identity of SERCA and the Golgi  $\text{Ca}^{2+}$ -ATPase is 33% and the function is very similar to that of SERCA, suggesting that they may be considered orthologues [certain homologues (genes with related DNA sequences) can be labelled more precisely: a paralogue is a different gene in the same species, structurally related but divergent in sequence, originating from gene duplication; an orthologue is a gene that is the closest functional and structural homologue in a different species]. The identity between SERCA and Na,K-ATPase is almost the same. The fact that the Na,K-

ATPase representative of type IIc is more similar to type IIa  $\text{Ca}^{2+}$ -ATPases than are type IIb  $\text{Ca}^{2+}$ -ATPases has been recognized [9], although phylogenetic-tree analysis did not produce this distinction [12].

The close relationship suggests the hypothesis that the SERCA  $\text{Ca}^{2+}$ -ATPase and the Na,K-ATPase have the same fold. To examine this possibility, we will look first at the linear alignment and then at some identified sites on the Na,K-ATPase to see if observations in the literature are consistent with a shared fold. Several sites on the homologous gastric H,K-ATPase will also be considered.

### LINEAR ALIGNMENT OF SERCA AND Na,K-ATPase

Figure 5 shows the linear alignment of rabbit SERCA1a and rat Na,K-ATPase  $\alpha 1$  produced by DDV, the alignment feature of Cn3D. Amino acids that do not align are in lower-case letters and are shown with gaps in the other sequence. The output of the program has been modified to show the numbering of each sequence, and the colouring scheme from Figure 1 is used to delineate the different domains. Later Figures will refer to some of the details. The yellow blocks are positions of transmembrane  $\alpha$ -helices, not taken from hydropathy plots, but transcribed from the SERCA structure (the position of the lipid bilayer can be roughly inferred from a low density of water molecules in the crystal [1]). Four of these helices extend well into the cytoplasm, and these extensions (the stalk segments, S2, S3, S4 and S5) are indicated with a lighter shade of yellow.

### HOMOLOGY AND HYDROPHOBICITY

The principal source of controversy in the predicted topologies of various transport ATPases has been hydropathy plots. Such plots have been highly successful in predicting transmembrane spans in proteins with no transport role or that transport only protons, but their application to Na,K-ATPase and its relatives has resulted in conflicting models for the arrangement of the C-terminal end of the protein. Examination of the SERCA structure reveals that there are actually quite a few polar residues buried in the membrane and a number of hydrophobic residues in the connecting short loops, and this complicates hydropathy analysis. The principal advantage of using gapped-BLAST for alignment is that it ignores hydrophobicity and gives equivalent consideration to all amino-acid-sequence homology, utilizing probability relationships derived from the analysis of evolutionarily related proteins. The outcome (Figure 5) is a credible alignment of all ten transmembrane spans and of the connecting short loops in the C-terminal end. Even the longest C-terminal loop, L7–8 (which extends out from the rest of the protein on the luminal face) aligns with the corresponding sequence in the Na,K-ATPase, except that the Na,K-ATPase has short deletions at each end that would bring the rest closer to the membrane. The most significant discrepancy in alignment of transmembrane spans is in M7: in Na,K-ATPase it is preceded by one short insertion and interrupted by two more, although the remainder nonetheless contains seven identical and six highly conserved residues. M2, M4 and M8 also appear to be shorter in Na,K-ATPase.

The residues that ligate  $\text{Ca}^{2+}$  in the SERCA structure are largely conserved in the Na,K-ATPase (Figure 5). Presumably the size of the ion-binding pocket, and its capacity for two  $\text{K}^+$  or three  $\text{Na}^+$  ions, is controlled by the spacing of the transmembrane spans, which in turn is controlled by other amino acids and the conformation changes occurring during transport. The con-



with mapped epitopes also gave topologies consistent with the aligned structure, once epitopes were determined with confidence [31–42]. An exception is the extracellular monoclonal antibody VG2, which has an epitope that should be intracellular in the structure. It either has a more complex epitope than originally thought [43], or it may detect conformational instability of the M5–M6 hairpin [44–46].

## TOPOLOGY

Efforts to determine topology with invasive molecular methods such as epitope insertion and  $\beta$ -galactosidase fusion proteins gave less consistent results for Na,K-ATPase topology. Some epitope insertions were consistent with the SERCA model, including those at Ala<sup>9</sup>, Met<sup>827</sup> and Pro<sup>1008</sup> [47]; Glu<sup>117</sup>, Lys<sup>828</sup>, Gln<sup>900</sup> and Val<sup>939</sup> [48]; and Ser<sup>114</sup>, Arg<sup>168</sup> and Leu<sup>313</sup> [49]. Other insertions gave topologies incompatible with the SERCA structure: Arg<sup>936</sup> and Leu<sup>973</sup> [47]; Phe<sup>876</sup> and Thr<sup>981</sup> [49]; and Leu<sup>973</sup> [50]. Note that one laboratory numbered residues from the prosequence of rat  $\alpha 1$  [47,49], and so numbers in their papers are larger by 5. The insertion at Phe<sup>876</sup> was found inside, but the site is projected to actually be within M7 near the extracellular surface. Arg<sup>936</sup>, which was found outside, is projected to be in the L8–9 loop, and is adjacent to the protein kinase A site; a protein-chemistry approach found Leu<sup>943</sup> (equivalent to Phe<sup>940</sup> in rat  $\alpha 1$ ) on the cytoplasmic surface [51]. Thr<sup>981</sup>, which was found inside, is projected to be at the extracellular end of M10. Leu<sup>973</sup>, which was found inside by two groups of investigators, is projected to be in the L9–10 extracellular loop. These insertions had a low transfection efficiency when it was studied, and so it seems likely that there was some interference with normal folding. Similar epitope insertions were made in the gastric H,K-ATPase [52]: insertions at Leu<sup>844</sup> (equivalent to rat  $\alpha 1$  Arg<sup>829</sup>) and Pro<sup>898</sup> ( $\alpha 1$  Glu<sup>883</sup>) gave topologies consistent with the SERCA model, but an insertion at Phe<sup>996</sup> ( $\alpha 1$  Pro<sup>980</sup>) should be at the extracellular end of M10, but was displayed at the intracellular surface instead.

When topology was studied by making fusion proteins with  $\beta$ -galactosidase as a reporter enzyme, topology consistent with the SERCA model was obtained for fusions at Arg<sup>62</sup> (N-terminal A domain), Glu<sup>118</sup> (extracellular loop L1–2), Ala<sup>249</sup> (L2–3 A domain), Leu<sup>313</sup> (extracellular loop L3–4), Ile<sup>948</sup> (intracellular loop L8–9), and Arg<sup>974</sup> (extracellular loop L9–10) [53]. Results suggesting an inverted orientation were obtained with fusions in the M5–M7 region, however: inside for a fusion at Ala<sup>791</sup> (projected to be in the extracellular L5–6 loop), outside at Met<sup>811</sup> (in M6, near the cytoplasmic side), and inside at Asp<sup>886</sup> (extracellular loop L7–8). The same results were obtained with expression in either bacteria or yeast. The authors interpreted the data as evidence for a different assignment of M5 and M6, and for a re-entrant P loop in L7–8, analogous to those in the mouth of ion channels. In view of the alignment of Na,K-ATPase with the SERCA structure, however, it now seems more likely that the discrepancies were due to the special folding requirements of the M5–M8 portion of the Na,K-ATPase, which does not follow conventional signal-anchor/stop-transfer rules [54,55]. Fusion proteins unable to form M5–M6 and M7–M8 hairpins for insertion may have given anomalous results.

Related to the proposal that L7–8 could extend through the membrane and be exposed on the other side [56], there have been reports that both the native SERCA's L7–8 loop and that of Na,K-ATPase were exposed on the cytoplasmic surface under some experimental conditions [14,43,57]. In the case of the

Na,K-ATPase, data on the binding of monoclonal antibody IIC9 have been interpreted to indicate detergent effects on the exposure of a site that was really always on the extracellular surface [39]. This is also consistent with the proximity of the epitope to the site of interaction with the Na,K-ATPase  $\beta$  subunit [58–60]. The two-sided exposure of the SERCA epitope 877–888 may have a similar explanation, in that effects of non-solubilizing detergent concentrations were seen [14], but the interpretation is not yet completely clear.

It must be remembered that the SERCA crystal structure represents just one conformation of the protein, and as with all crystals of proteins with flexible domain interactions, it could even be distorted by crystal packing forces. It remains technically possible that the transmembrane spans rearrange significantly during catalysis. The analysis presented here also does not take into account the likely locations of the Na,K-ATPase  $\beta$  and  $\gamma$  subunits [42]. In view of the crystal structure, however, the possibility that L7–8 could form a re-entrant loop seems remote.

The disposition of water molecules in the SERCA crystal structure suggested the position of the lipid barrier [1]. However, it should be noted that the boundaries between aqueous and lipid phases are still not known with any accuracy, and they may differ between conformations.

## PROTEOLYTIC CLEAVAGE SITES

Proteolysis of SERCA, Na,K-ATPase and gastric H,K-ATPase has been a useful tool for developing models of protein arrangement. The proteins all show selective conformation-dependent cleavage at a few sensitive sites, and they also all show limit digestion of native enzyme in which the domain from M7 to the C-terminus (Figure 2) is resistant to further digestion [61–66]. On Figure 5, attention is drawn to some proteolytic sites that are shared by Na,K-ATPase and H,K-ATPase, and their locations on the SERCA structure are shown in Figure 6. Site (1) is a cluster of sites (for trypsin and chymotrypsin) on the extended link between the N-terminus and M1 [61,63,67–70]. The cleavage site lies in or near a proline-rich stretch that it also thought to be the site of binding of an SH3 domain protein (see below). On SERCA the equivalent site (which is moderately well conserved, but has only one proline residue) is highly exposed. Site (2) (trypsin) [71,72] is on the extended segment linking M2 to the A domain, and site (3) (closely spaced trypsin and chymotrypsin sites on Na,K-ATPase, or trypsin and papain sites on H,K-ATPase; two arrows) [61,63,68,72] is on the extended segment linking the A domain to M3. Site (4) (trypsin for Na,K-ATPase, and trypsin or a nearby papain site for H,K-ATPase) is interesting, because it is the beginning of the soluble N domain fragment that can be isolated from all three ATPases [73–76]. Similar N domain fragments capable of folding and binding nucleotides have also been produced by expressing and reconstituting fragments of the same region [77–79]. Sites (5), (6) and (7) are tryptic sites that have been called 'T1', 'T1'' and 'T4' [34]; T1 is the most readily cleaved site on the enzyme, and is exposed preferentially in K<sup>+</sup> [80]. Extensive digestion, or digestion after some structural perturbation, produces several additional cleavages in the P domain preceding M5, but these sites are not shown on the Figure because their exposure in native enzyme is unlikely. Site (7) is the probable end of the soluble N domain fragments, trypsin (T4) for both enzymes and a nearby papain site for H,K-ATPase. Site (8) (trypsin, chymotrypsin and pronase) is the beginning of the protease-resistant C-terminal domain that was originally called the '19 kDa fragment'

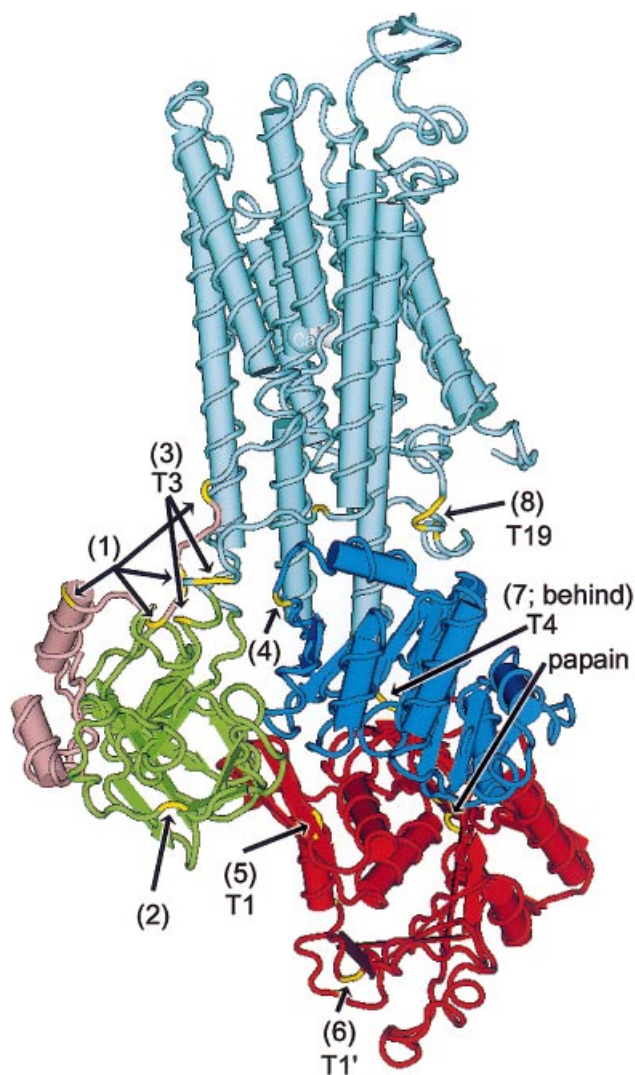


**Figure 6** Na,K-ATPase and H,K-ATPase proteolysis site locations

In this and most of the rest of the Figures, the SERCA structure is shown, but features of Na,K-ATPase are aligned and identified on it to test whether the alignment is credible. This Figure shows the principal sites of proteolysis of Na,K-ATPase and gastric H,K-ATPase. All of the sites have appropriate surface exposure.

[61–63,66,68,71,72,81]. It is exposed to protease only after digestion of other sites in the cytoplasmic domains. All of the projected positions of Na,K-ATPase and H,K-ATPase cleavage site are on the surface (Figure 6), and support the similarity with the SERCA structure.

One puzzling thing that has been observed for both Na,K-ATPase and H,K-ATPase is the apparent accessibility of the L9–10 extracellular loop on the cytoplasmic surface in some experimental circumstances [52,63,71]. In other digestion experiments, the expected M9–M10 loop was not recovered [64,72]. This may be related to the thermal lability of the C-terminal end of the protein [42,82,83]. M9 and M10 may slip out of the membrane to either side after structural perturbation, such as cleavage at other sites. M5–M6 can also slip out of the membrane after digestion [44,45,84].

## GAPS AND INSERTIONS

When two proteins have the same fold but also have significant sequence divergence, it is common for insertions to be present in the form of loops at the surface. As seen in Figure 5, the gapped-BLAST alignment of SERCA and Na,K-ATPase detects a number of gaps and insertions. Figures 7(A) and 7(B) illustrate the portions of SERCA that are insertions relative to Na,K-ATPase, using the Cn3D display mode called 'weighted variety'. In this colour mode, as in Figure 3 and 4, grey means that the two sequences could not be aligned at all. The rest of the residues are colour-coded for degree of similarity: the reddest residues are identical, the bluest are not conserved at all, and in between are two shades of purple representing highly conserved and less conserved substitutions. The spacefill style, in which the individual atoms are shown rather than the underlying secondary structure, makes the superficial positions of the insertions more visible. The identified insertions (stretches not present in Na,K-ATPase) are labelled. Most of the grey loops begin and end very close together, consistent with their deletion in Na,K-ATPase without major alteration in the underlying fold. One exception is illustrated below in Figure 9.

Figures 7(C) and 7(D) illustrate some of the points at which Na,K-ATPase has insertions relative to SERCA. Here the two residues of SERCA that flank each insertion were highlighted with yellow. Again, all of these points (for insertions of four or more amino acids) were at the surface, with one major exception. Figure 7(C) shows four insertion points in the N and P domains that are all at the surface. Figure 7(D) shows two insertion points in M7 that would be more disruptive, presumably adding extra turns to the helix. These insertions are in the cytoplasmic half of the span, suggesting that, in the Na,K-ATPase, M7 extends further into the cytoplasm. Two additional insertions preceding M7 are also shown. Since M7 is at the edge of the bundle of  $\alpha$ -helices, the insertions could be expected to be accommodated without disrupting the overall fold. We can speculate, on the basis of these unique insertions and other considerations, that the Na,K-ATPase  $\beta$  subunit associates with the complex near M7 and M8 [42].

The most obvious place where Na,K-ATPase and SERCA do not align is at the N-terminus. In the SERCA crystal structure, the N-terminal portion of the A domain consists of two short  $\alpha$ -helices at the surface of the protein, and an extended link to M1. The break between the two  $\alpha$ -helices is the sequence **GVSETTGLTP**, and the corresponding sequence in Na,K-ATPase is the homologous **GTDLRGLTP**, which strongly suggests that the two proteins have the same two-helix motif (Figure 8). Curiously, the other class of  $\text{Ca}^{2+}$ -ATPases, PMCA and the proton pump of *Neurospora*, align with SERCA starting with the second helix. At the location of the break between the helices, the *Neurospora* enzyme has the sequence **QTDTRVGLTS**, and PMCA has **SPNEGLSGNP**. Finally, the mature form of rat  $\alpha 1$  Na,K-ATPase has 34 extra amino acids at the N-terminus, which includes the protein kinase C phosphorylation sites (**SEHGDKKSKK**). No corresponding structure is found in SERCA, but because of its location relative to the SERCA structure, this phosphorylation site should be well-exposed. It is notable that there is great sequence variation at the N-terminus even within the Na,K-ATPase subfamily, making a conserved structure there unlikely.

One other notable difference between SERCA and Na,K-ATPase entails the location of the phospholamban-binding site. Phospholamban is a 52-amino-acid single-span membrane protein that regulates SERCA [85]. It was not present in the crystallized SERCA1a from skeletal muscle, since it is expressed

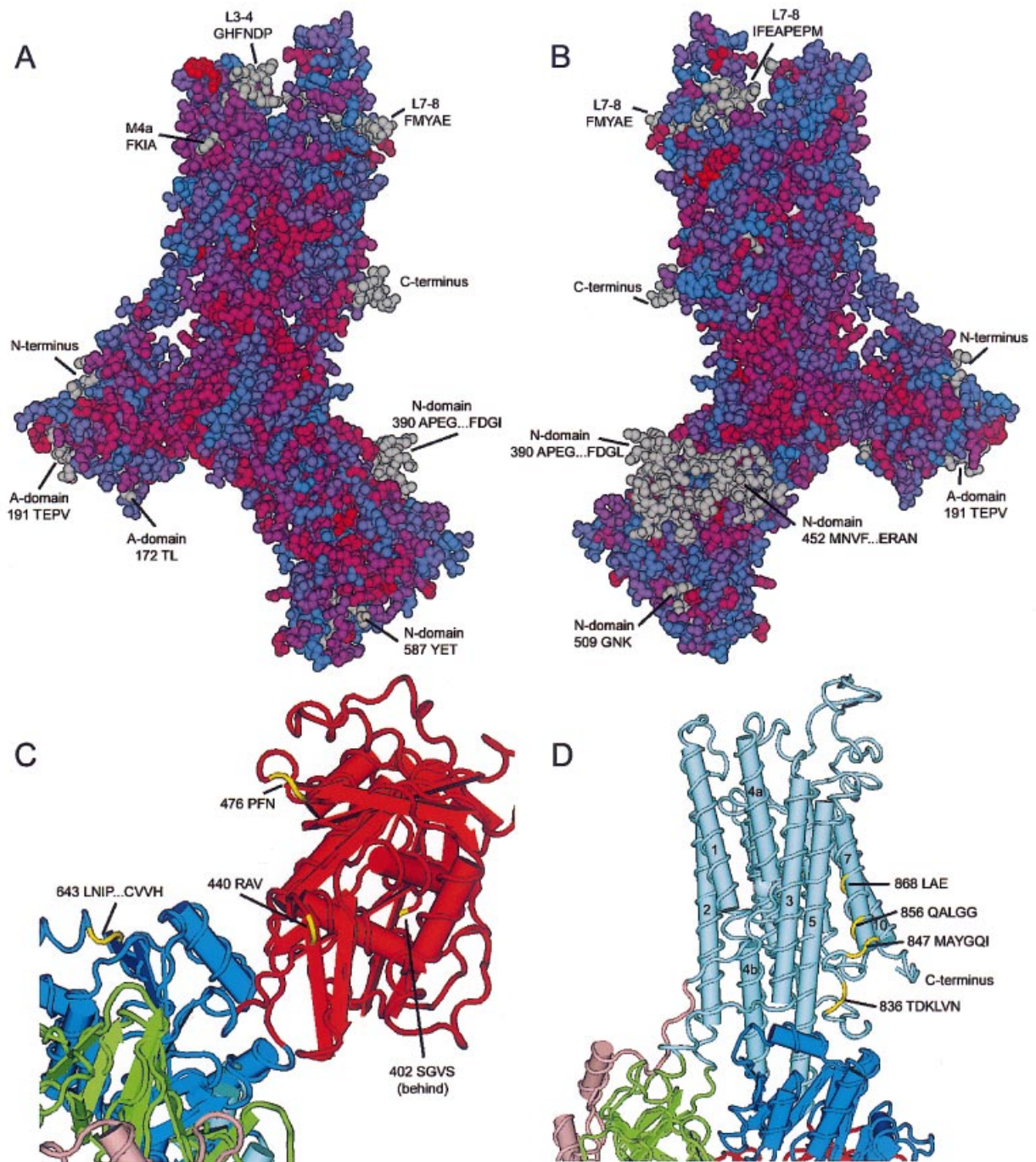


**Figure 7** SERCA and Na,K-ATPase differences in surface loops

As seen in Figure 5, there are places where there are insertions and deletions when SERCA and Na,K-ATPase are compared. (A) and (B) show in grey the SERCA sequences that are deleted in Na,K-ATPase: almost all deletions of more than three residues are at the surface. (C) and (D) show in yellow sites where Na,K-ATPase has insertions that are not present in SERCA. In (C), four representative sites in the N and P domains are all at the surface. In (D) one of two problem areas is highlighted: insertion sites in M7 that may be more disruptive. Note, however, that elongation of M7 may be accommodated without disrupting the fold.

predominantly in cardiac muscle with the very similar SERCA2a isoform. The exact position of phospholamban in the enzyme is not known with certainty, but certain mutations of M6 were observed to affect phospholamban association [86], and cross-linking, chimaeras and site-directed mutagenesis led to the identification of a six-amino-acid stretch at 397–402 in the N-

domain that is critical [87,88]. Figure 9(A) shows all of these residues in secondary-structure view. Of the residues in M6, only the residues closer to the cytoplasm, namely Leu<sup>802</sup>, Thr<sup>805</sup> and Phe<sup>809</sup>, are exposed in this conformation, and they are recessed between M2 and M9. It seems likely that a more comprehensive search for phospholamban-contacting residues will find contri-

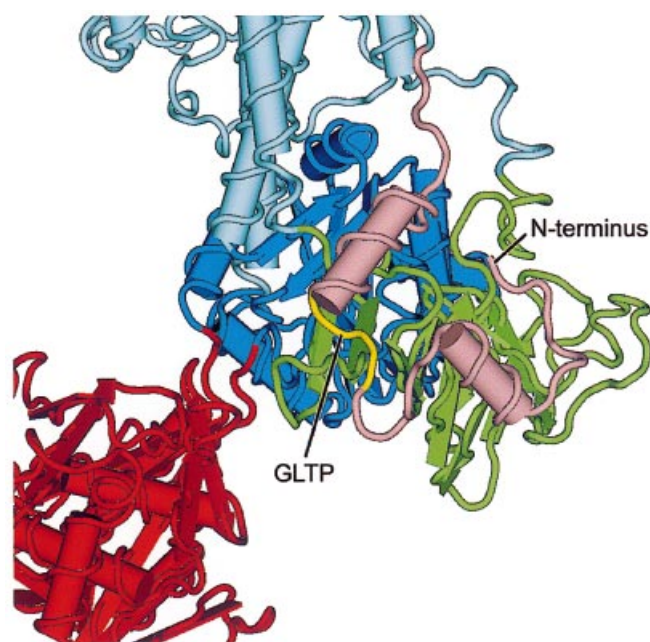


**Figure 8** The break between the A domain helices

In the N-terminal portion of the SERCA A domain (pink) there are two  $\alpha$ -helices broken by the sequence GLTP. The same sequence is conserved in Na,K-ATPase, supporting the likelihood that it has the same fold at that position.

butions from other transmembrane spans. The more intriguing observation is that the N domain site (KDDKVI in SERCA2; KNDKPI in SERCA1a) (highlighted yellow in Figures 9A and 9B) is on one of the surface regions that is present in SERCA but not in Na,K-ATPase. This is the same region that is labelled 'N domain, APEG...FDGL' in Figure 7(A) and 7(B). The 21-amino-acid segment that is absent in Na,K-ATPase is one of the few that does not begin and end neatly at the same location in the SERCA structure (Figure 9C). This means that the N domain structure has to differ between the two ATPases to accommodate the absence of these residues. Na,K-ATPase has its own single-span regulator (the  $\gamma$  subunit), but it is unrelated structurally to phospholamban, and its binding site is not yet known [42].

### PREDICTED LOCATION OF CYSTEINE RESIDUES

Cysteine residues, because of their unique reactivity and ability to form disulphide bonds, are of particular interest in protein chemistry. The Na,K-ATPase has 23 of them, and a number have been the target of modification. Several were predicted to be in transmembrane spans or at the extracellular surface. Since the gapped-BLAST alignment with the SERCA structure calls for adjustments to the predicted transmembrane spans, it is useful to re-examine the positions of those cysteine residues. Figure 10(A) shows all of the natural cysteine residues in rat  $\alpha 1$  that were predicted to be in or near the membrane. These cysteine residues have been mutated as a group by Arguello and associates [89], generating enzyme free of extracellular and membrane cysteine residues that can be expressed in HeLa cells, and that has no alteration of  $\text{Na}^+$  or  $\text{K}^+$  apparent affinity. All 23 cysteine residues have been eliminated by Kaplan and associates, creating an enzyme that can still be expressed with activity in insect cells [90]. Both of these constructs should be valuable for further structural studies.

In Figure 10(A), two significant differences from the traditional predicted cysteine locations can be seen. Cys<sup>104</sup> (Cys<sup>106</sup> in rat; Cys<sup>113</sup> in *Xenopus*) was originally thought to be in the middle of M1. It was somewhat surprising that its mutation reduced ouabain binding [91], and that it reacted with a derivative of digoxigenin [92,93] and with extracellular mercury [94,95]. It was even proposed that M1 could be part of a ouabain-binding cleft [96]. The corresponding position in SERCA, however, is one turn from the top of M1, and, because M1 sticks out a little more than surrounding  $\alpha$ -helices, this cysteine may be accessible to the extracellular medium. The other difference was the position of Cys<sup>964</sup>, the site at which the fluorescent probe BIPM {N-[p-(2-benzimidazolyl)phenyl]maleimide} binds to the Na,K-ATPase [97,98]. It was originally predicted to be in the middle of M9, which was puzzling in view of BIPM's reactivity and usefulness as a reporter of enzyme conformation. However, Cys<sup>964</sup> has recently been shown to be accessible both to SDSM (4-acetamidomaleimidylstilbene-2,2'-disulphonic acid) [26] and to  $\text{Hg}^{2+}$  [95] from the extracellular surface. In agreement with the conclusions of Lutsenko et al. [26], the projected location is at the extracellular end of M9. Cys<sup>911</sup>, which was somewhat less reactive to SDSM, should also be extracellular, at the end of M8. Both Cys<sup>911</sup> and Cys<sup>964</sup> showed conformation-dependent changes in reactivity [26,95]. Certain residues between SYGQ and Cys<sup>911</sup> have been implicated in interaction between Na,K-ATPase  $\alpha$  and  $\beta$  subunits [99], which may be further evidence for an exposed extracellular position.

Cysteine residues introduced into the Na,K-ATPase  $\alpha$  subunit in the predicted extracellular loops have been used to test the topology model [28]. The two most reactive of the natural cysteine residues, Cys<sup>911</sup> and Cys<sup>964</sup>, were eliminated by mutation first. The introduced residues, namely Cys<sup>118</sup>  $\rightarrow$  Pro, Cys<sup>309</sup>  $\rightarrow$  Thr, Cys<sup>793</sup>  $\rightarrow$  Leu, Cys<sup>876</sup>  $\rightarrow$  Leu, and Cys<sup>973</sup>  $\rightarrow$  Met, reacted with extracellular N-biotinylaminoethyl methanethiosulphonate ('MTSEA-biotin'). Figure 10(B) shows the locations of the introduced cysteine residues mapped on to the SERCA structure. All residues except Leu<sup>876</sup> appear to be well-exposed in this conformation, and Leu<sup>876</sup> is in M7, the span with insertions that may make it extend further out of the membrane than in SERCA. Two residues introduced in the L9–10 loop at positions flanking Met<sup>973</sup> (Cys<sup>969</sup>  $\rightarrow$  Val and Cys<sup>976</sup>  $\rightarrow$  Leu) did not react with the reagent. In the structure, both of these are in L9–10, and the reason they did not react is not clear. The experimental evidence on Na,K-ATPase is thus largely consistent with homology with the SERCA structure.

Introduced cysteine residues have also been used to determine the accessibility of residues of M5 in both native enzyme and enzyme treated with palytoxin, a natural toxin capable of making the Na,K-ATPase act like a non-specific ion channel [100]. Only a cysteine residue at the position equivalent to Ala<sup>796</sup> of rat  $\alpha 1$  was reactive to a methanethiosulphonate derivative in native enzyme, and, when projected on to SERCA, this site is in the L5–6 extracellular loop, exposed to the medium. Several other introduced cysteine residues on M5 became accessible with palytoxin treatment.

Because omeprazole, a clinically useful inhibitor of gastric H,K-ATPase, reacts with cysteine residues at the enzyme surface, those residues have been mapped, and the principal candidates are in or near the extracellular L5–6, L3–4, and L7–8 loops [101]. Accessibility to several cationic sulphenamides followed by identification of the labelled fragments pointed to the accessibility of Cys<sup>321</sup>, Cys<sup>813</sup> or Cys<sup>822</sup> and Cys<sup>892</sup> [102]. On the SERCA structure, Cys<sup>321</sup> and Cys<sup>813</sup> are the only residues predicted to be exposed on the extracellular loops; Cys<sup>822</sup> would be well-buried in M6 and Cys<sup>892</sup> would be one turn from the top of M7 (not

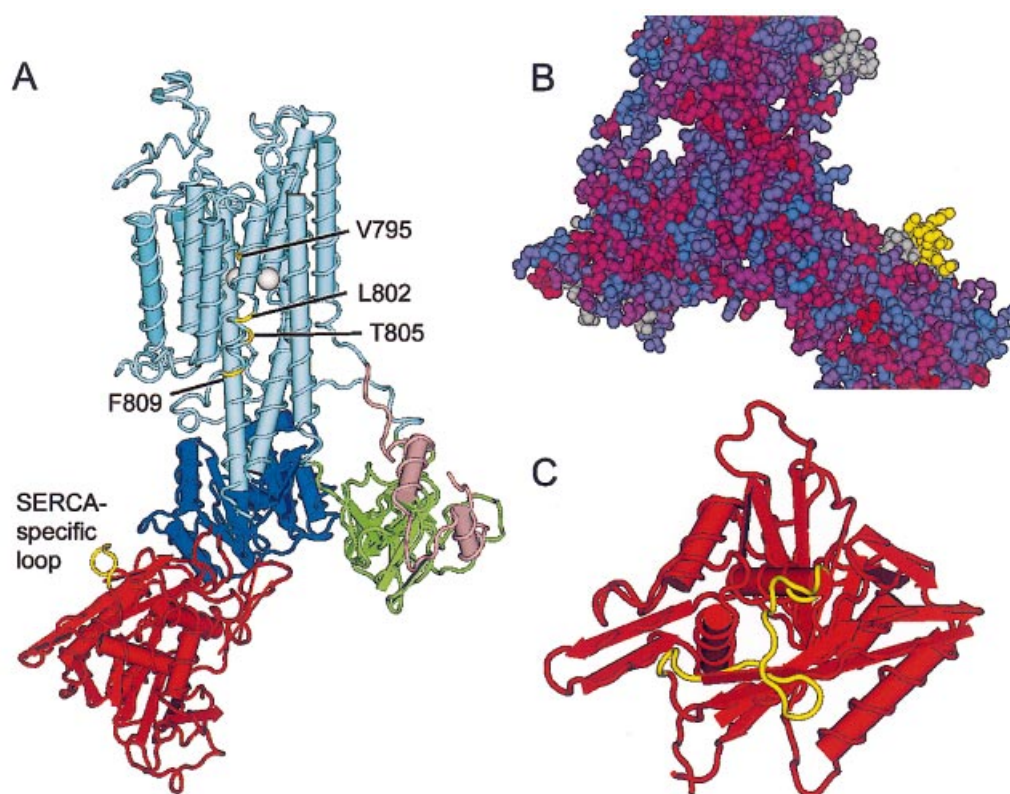


**Figure 9** Phospholamban binding sites on SERCA

Residues of SERCA that interact with SERCA's single-span regulator, phospholamban. In (A), four specific mutations in M6 were found to affect phospholamban binding (Val<sup>795</sup>–Phe<sup>809</sup>); in the SERCA structure, the lower three are exposed to some extent and could interact with phospholamban. The critical residues in a loop on the N-domain (yellow) are actually deleted in Na,K-ATPase. (B) shows the exposed position of this loop. (C) shows the deleted loop in yellow. This is the second problem area: the ends of the deletion are not very close, requiring some rearrangement of the N-domain fold in the Na,K-ATPase.

shown). Interestingly, site-directed mutagenesis of Cys<sup>813</sup> and Cys<sup>822</sup> indicated that only mutation of Cys<sup>822</sup> blocked inhibition by omeprazole [103]. Mutation of Cys<sup>813</sup> had marked effects on the affinity of another H,K-ATPase inhibitor, SCH 28080, however.

#### PREDICTED LOCATION OF CROSS-LINKS

Cross-linking between endogenous cysteine residues by oxidation to disulphide bonds has been attempted as a way to probe the organization of transmembrane spans in the Na,K-ATPase. Before discussing particular observations, it is useful to view the sites where cross-links have been formed in the SERCA enzyme itself (Figure 11). The endogenous transmembrane cysteine residues of SERCA were first removed by mutagenesis, and then pairs of cysteine residues were reintroduced into M4 and M6 to probe for interaction [104]. Cross-linking was carried out without detergent treatment. The geometry of the successful pairs was favourable when viewed on the SERCA structure. Cross-links formed most readily between residues 317 and 807 or 321 and 808 in M4 and M6 (Figure 11A); they formed with lower yield between residues 309 and 796 in the same segments (Figure 11B). This was interpreted as a greater separation caused by tilt in the relative orientation of the two helices, but Figure 11 shows a different interpretation. The proximity of the more-reactive and less-reactive pairs is not very different, but the less-reactive pair is more buried within the membrane, and therefore probably less

accessible to the oxidative catalyst, Cu<sup>2+</sup>-phenanthroline. Another identified, conformationally sensitive cross-link in SERCA is between Lys<sup>492</sup> and Arg<sup>678</sup> in the N and P domains respectively catalysed by glutaraldehyde (Figure 11C) [105]. In this conformation these sites are widely separated, but they presumably come together in the closed conformation [1,3,106].

The geometry of known and inferred oxidative cross-links in the Na,K-ATPase  $\alpha$  subunit does not look as favourable (Figure 12), but this may be due to the formation of otherwise-unlikely cross-links under conditions of atypical structural flexibility. The oxidative cross-linking studies grew out of the early work of Askari and his collaborators on cross-linking between subunits of Na,K-ATPase oligomers, in which the formation of links was dependent upon enzyme conformation, and in some cases, promoted by detergent treatment [107,108]. The more recent attempts to detect intra-subunit cross-links have depended on the ability to generate identified proteolytic fragments containing the transmembrane spans [81], and it is notable that the cross-links were formed after, not before, digestion. In digitonin- or deca(ethylene glycol) monododecyl ether (C<sub>12</sub>E<sub>10</sub>)-solubilized digested enzyme, oxidative cross-linking produced a link between the M1–M2 hairpin and the M7–M10 domain, and between this complex and the  $\beta$  subunit [109,110]. In digested enzyme that was not solubilized, the same M1–M2 to M7–M10 product was formed, but  $\beta$  subunit was found with it only if  $\beta$  was cleaved at a site on the extracellular side, implying that intact  $\beta$  was not close enough to cross-link without the detergent treatment [111].

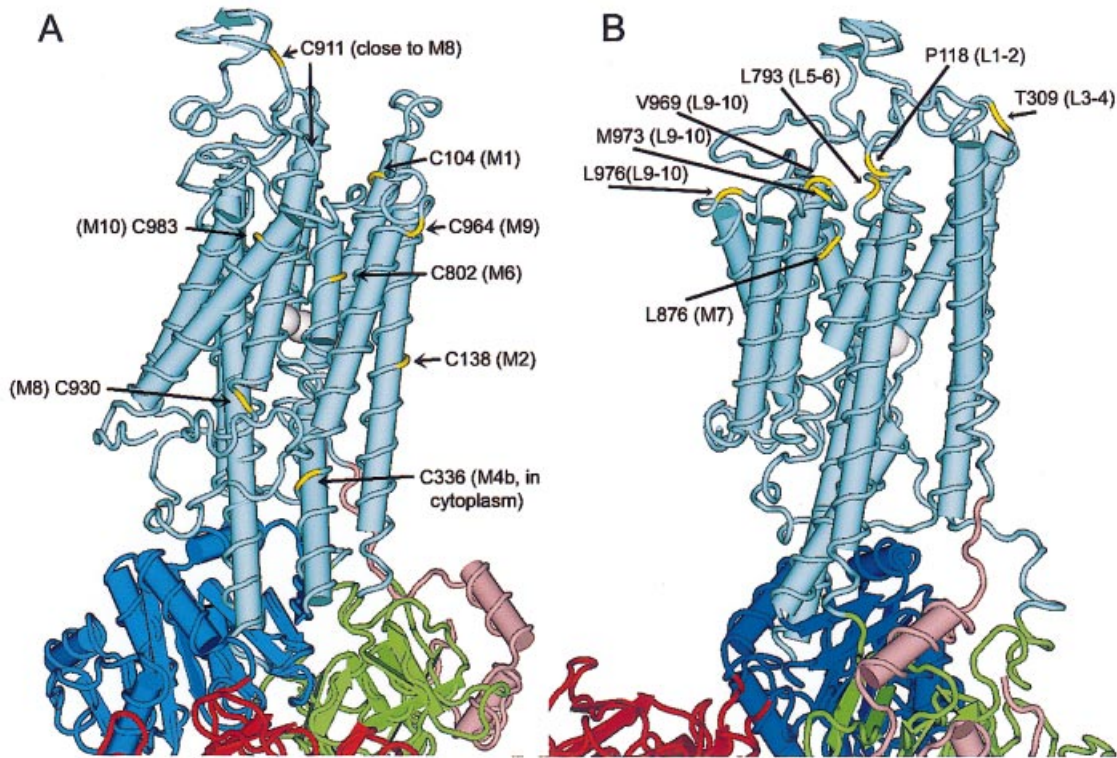


**Figure 10** Projected location of Na,K-ATPase cysteine residues

In this Figure the numbering of Na,K-ATPase residues is that of sheep  $\alpha 1$  (two shorter than the rat  $\alpha 1$  of Figure 5) because the relevant mutagenesis experiments utilized the sheep  $\alpha 1$  subunit [89,90]. (A) Shows the naturally occurring cysteine residues of Na,K-ATPase projected on to the SERCA structure with gapped-BLAST. (B) shows the cysteine residues that Hu and Kaplan [28] introduced into Na,K-ATPase. In agreement with their protein chemistry, the homologous sites are well exposed.

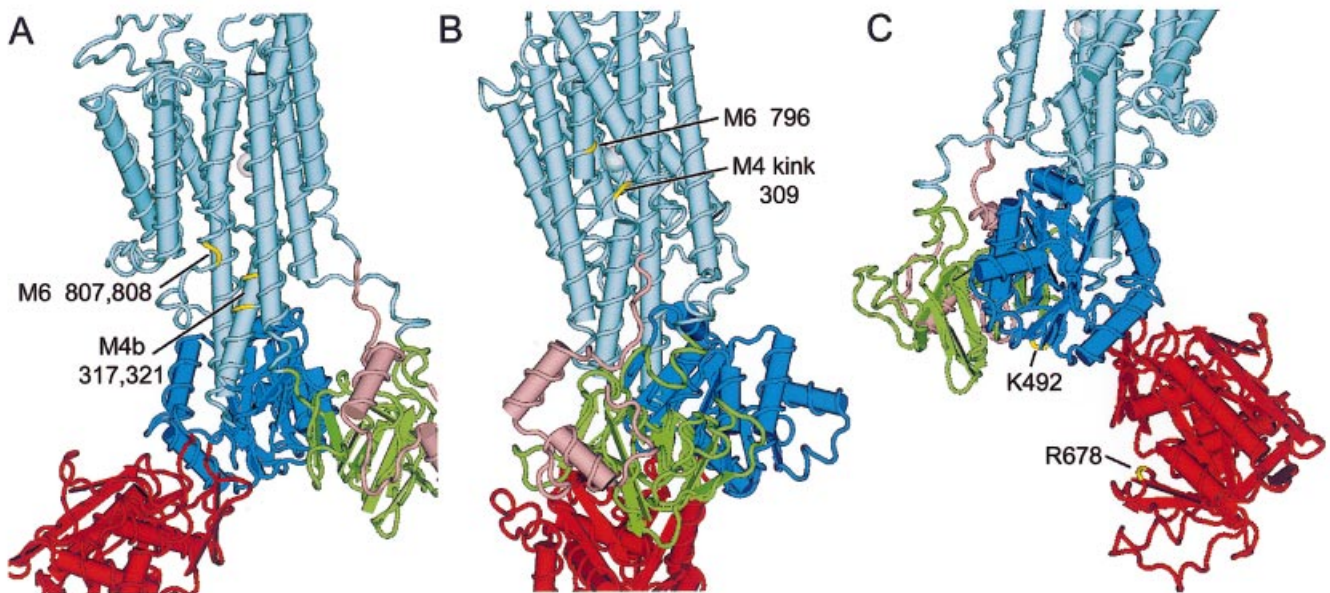


**Figure 11** Identified cross-linking sites in SERCA itself

(A) and (B) show two sites in SERCA where disulphide bonds can be formed between introduced cysteine residues. Proximity for the successful pairs is good. (C) Shows two residues shown to be cross-linked by glutaraldehyde treatment. Their cross-linking supports large inter-domain movements between the P (blue) and N (red) domains.

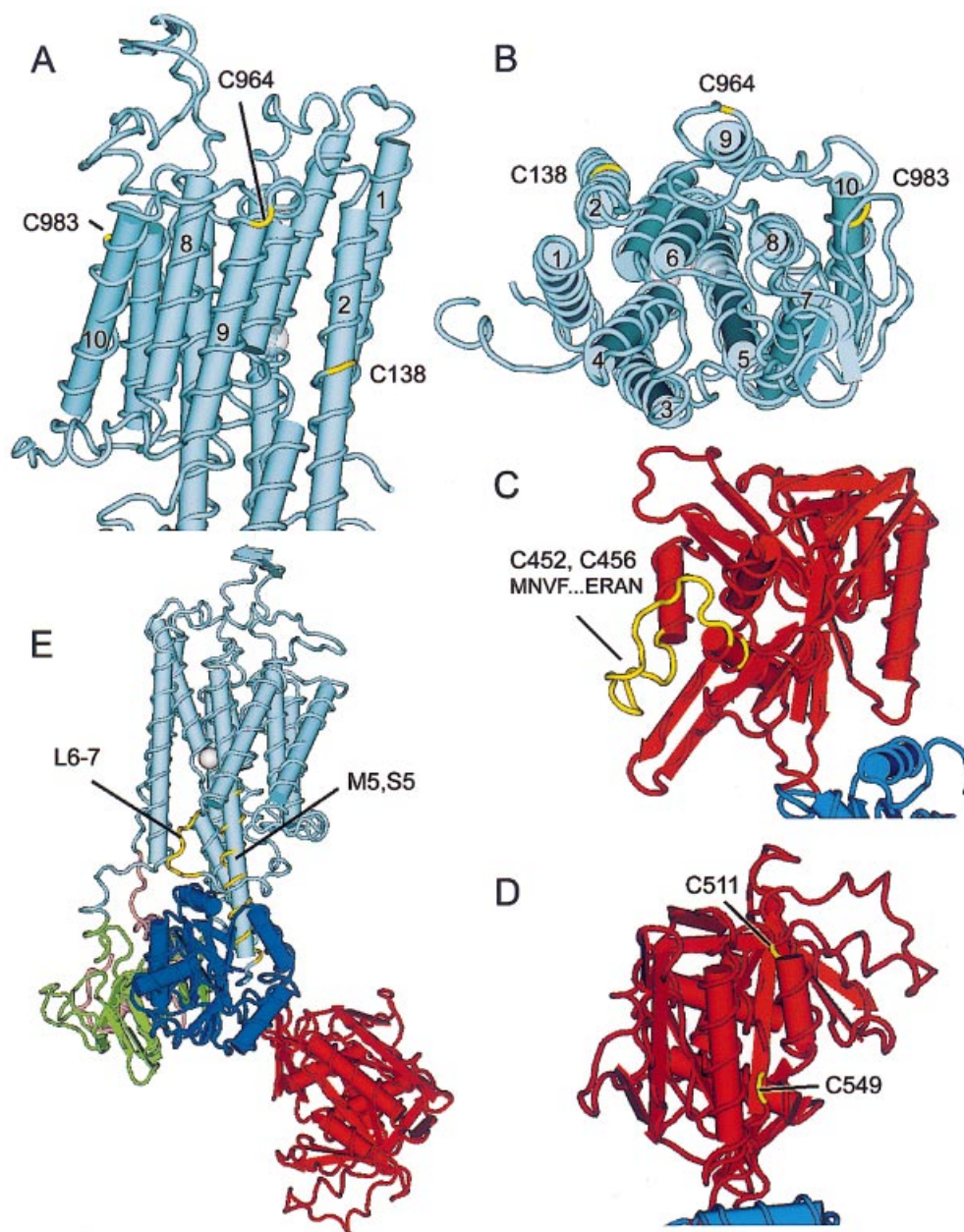


**Figure 12** Cross-linking sites in Na,K-ATPase projected on to the SERCA structure

(A) and (B) show the predicted positions of cysteine residues that are likely to be cross-linked by oxidation of disulphides. Proximity is not particularly good, which may explain why cross-linking requires detergent treatment or proteolysis to proceed in reasonable yield. (C) and (D) show the only spontaneously formed oxidative cross-links detected in native Na,K-ATPase, both in the N domain. The numbering for rat would be two higher. One occurs at the ends of a surface loop (yellow) that is deleted in Na,K-ATPase (C). The other pair does not show very good proximity in the SERCA structure (D). (E) shows the location of two regions cross-linked by  $\alpha$ -phthalaldehyde.

Cross-linking in the membrane-bound digested enzyme was inhibited by the presence of  $\text{Na}^+$ ,  $\text{K}^+$  and ouabain [111]. This was interpreted such that the interactions of these ligands with the digested enzyme modify the three-dimensional packing of the transmembrane helices [111]. Others have shown that these ligands serve to stabilize the complex of digested membrane fragments against thermal denaturation [61,63], which suggests the related hypothesis that formation of cross-links may have required some structural perturbation. Spontaneous cross-link-

ing was observed in  $\text{C}_{12}\text{E}_{10}$ -solubilized digested enzyme, but the catalyst  $\text{Cu}^{2+}$ -phenanthroline was required for the membrane-bound enzyme [110].

The cross-link between M1–M2 and M7–M10 has not been definitively identified because of low yields [110,112]. In examining the positions of Na,K-ATPase cysteine residues with respect to the SERCA structure, the best proximity would appear to be between Cys<sup>138</sup> in M2 and Cys<sup>964</sup> in M9 (Figures 12A and 12B). In Figure 12(B), M4b appears to come between

M2 and M9, but it is actually below them, in the cytoplasm. Some rearrangement of membrane spans to bring the residues closer together would be needed to link M1–M2 to M7–M10. The formation of this cross-link was first detected when the digested complex was solubilized in the absence of stabilizing ligands [109], and that combined with low yield in the presence of stabilizing  $\text{Rb}^+$  [110], is consistent with a sub-optimal orientation of sites.

Further identification of the cross-linked segments after chymotrypsin [110] or CNBr cleavage [112] narrowed down the possible cysteine residues involved, and more evidence was obtained for the nature of the cross-link between the  $\alpha$  and  $\beta$  subunits [110,112], which appears to be between Cys<sup>44</sup> of  $\beta$  and either Cys<sup>911</sup> or Cys<sup>930</sup> of  $\alpha$ . These two residues on  $\alpha$  are most likely at the extreme ends of M8: Cys<sup>911</sup> at the extracellular surface and Cys<sup>930</sup> at the intracellular surface [26]. Thus the apparent need to either solubilize the complex in detergent or to digest the  $\beta$  subunit at the extracellular surface could permit the  $\beta$  subunit to either ascend or descend in the membrane to form a cross-link to one of these cysteine residues. Ivanov et al. stated “... Evidently some backbone flexibility induced by detergent solubilization is required for close juxtaposition of the Cys44 of  $\beta$  with one of the nearby intramembrane cysteines of  $\alpha$  to allow the disulfide bridge formation ...” [112].

In addition, there is evidence for a cross-link between Cys<sup>964</sup> and Cys<sup>983</sup> (M9 and M10) [110,112]. Figures 12(A) and 12(B) show the disposition of these two residues mapped on to the SERCA structure. They do not look very favourably oriented for intramolecular cross-linking in this conformation, but at least they are both at the same end of the helix bundle, and a relatively simple rotation could bring them closer. Future research using introduced cysteine residues based on the SERCA model may provide better cross-linking and more satisfactory interpretations.

Gevondyan et al. reported finding spontaneously formed disulphide bonds in the  $\alpha$  subunit on the intracellular side of the membrane [113] between Cys<sup>452</sup> and Cys<sup>456</sup>, and between Cys<sup>511</sup> and Cys<sup>549</sup>. In the SERCA structure, the equivalent positions of 452 and 456 (454 and 458 in rat) are at either end of an insertion in SERCA, the loop from MNVF to ERAN on the N domain (Figure 12C); the proximity should be favourable for forming a disulphide. The other disulphide occurs at two residues that are only moderately close in the SERCA structure, but they are in a part of the N domain that may be rearranged in Na,K-ATPase (compare with Figure 9C). Disulphides found in purified enzyme do not necessarily occur in the reducing environment of the cell, and it has been demonstrated that mutation of these residues does not inactivate the Na,K-ATPase [89,114].

The last example of an identified cross-link site (Figure 12E) is from Ala<sup>749</sup> to Ala<sup>770</sup> of the P domain just before the M5–M6 hairpin to Asn<sup>831</sup>–Arg<sup>841</sup> of the L6–7 intracellular loop, close to T19 (Figure 6), where trypsin cleaves to generate the M7–M10 tryptic fragment. This link was formed by reaction with *o*-phthalaldehyde in digested or digested and solubilized enzyme in the presence of  $\text{Rb}^+$  [59]. When these regions are highlighted on the SERCA structure, they are quite close. There is evidence for the importance of the L6–7 loop in conformation change in both Na,K-ATPase and SERCA itself [1,115,116].

### PROXIMITY RELATIONSHIPS FROM METAL-ION CLEAVAGE

Some unique insights into interdomain movements in the Na,K-ATPase have come from the exploitation of the fact that bound metal ions such as  $\text{Fe}^{2+}$ ,  $\text{Fe}^{3+}$ , or  $\text{Cu}^{2+}$  can catalyse specific

protein cleavages in the immediate vicinity of the metal, under oxidative conditions [117]. For Fe cleavage, several protein fragments were obtained with the same time course and concentration-dependence, suggesting cleavage of spatially clustered loops on the cytoplasmic surface. One bound Fe atom resulted in the cleavage of three sites in the P domain and one in the A domain in a conformation-dependent manner: cleavage occurred in E2 but not in E1. The sites cleaved were all highly conserved among P-type ATPases, supporting their importance as structural elements critical for conformation change, brought together in only one conformation. Cleavage at a second site near the membrane interface was not affected by conformation.  $\text{Mg}^{2+}$  and  $\text{P}_i$  were shown to non-competitively prevent the Fe-catalysed cleavage in the P domain, presumably by preventing Fe binding, and leading to prediction of sites involved in binding of each of these ligands [118], nor far from sites supported by site-directed mutagenesis [119–121]. ATP forms a complex with Fe that, in turn, can be used as an affinity reagent for the active site. Because cleavage only occurred in conformations with high-affinity ATP binding (E1 and E1Na), the sites partially differed from those in E2 with Fe alone [122]. Furthermore, differences were noted in E1P and E2P, strongly supporting large conformation-dependent domain movements. In E1, N is predicted to dock on to P with A moved off to one side, whereas, in E2(K), A is predicted to dock on to P and N is displaced. The data also predict a shift in  $\text{Mg}^{2+}$  binding from the P domain to the N domain. Much more detail and useful diagrams can be found in a review [123] by the above-cited authors.  $\text{Cu}^{2+}$  was observed to catalyse cleavages at the opposite surface in extracellular loops of  $\alpha$  and in the  $\beta$  subunit [27]. All of the data are consistent with the SERCA1a crystal structure, and in fact support the emerging model of how the pump works.

### BINDING SITES FOR OTHER PROTEINS

Proteins with known specific binding sites on the Na,K-ATPase include protein kinases C and A, the cytoskeletal protein ankyrin, and an SH3-domain-containing protein, phosphoinositide-3 kinase. The likely locations of the binding sites for protein kinase C and A have been reviewed elsewhere [124]. The protein kinase C site is on the N-terminal extension of Na,K-ATPase that has no corresponding segment in SERCA, and, with its high density of charge, it is anticipated to be well-exposed. The predicted location of the protein kinase A site is very close to the membrane and rather hidden, which appears to explain why Na,K-ATPase cannot be phosphorylated by protein kinase A *in vitro* unless it is treated with detergent. An outstanding question is how activation of protein kinase A produces the various activating and inhibiting effects on Na,K-ATPase that are seen in cells.

Ankyrin, which is involved in restricting the distribution of Na,K-ATPase to particular membrane regions in some cells, binds with the highest affinity to a site on the L2–3 intracellular loop (Ser<sup>142</sup>–Val<sup>166</sup>) [125,126]. On SERCA, this site is highly exposed on the segment that links the A domain to M2 (Figure 13A). A lower-affinity site was also identified in the large L4–5 intracellular loop [127], but on SERCA this site is quite buried within the N domain (Figure 13B). However, the sequence (ALLK) is adjacent to a loop that is deleted in Na,K-ATPase and adjacent to the site of the disulphide bond detected by Gevondyan et al. (Figure 12C), and so it is conceivable that the Na,K-ATPase structure is altered enough to expose the site. ALLK is homologous to the sequence ALLLK which participates in ankyrin binding in anion exchanger 1.

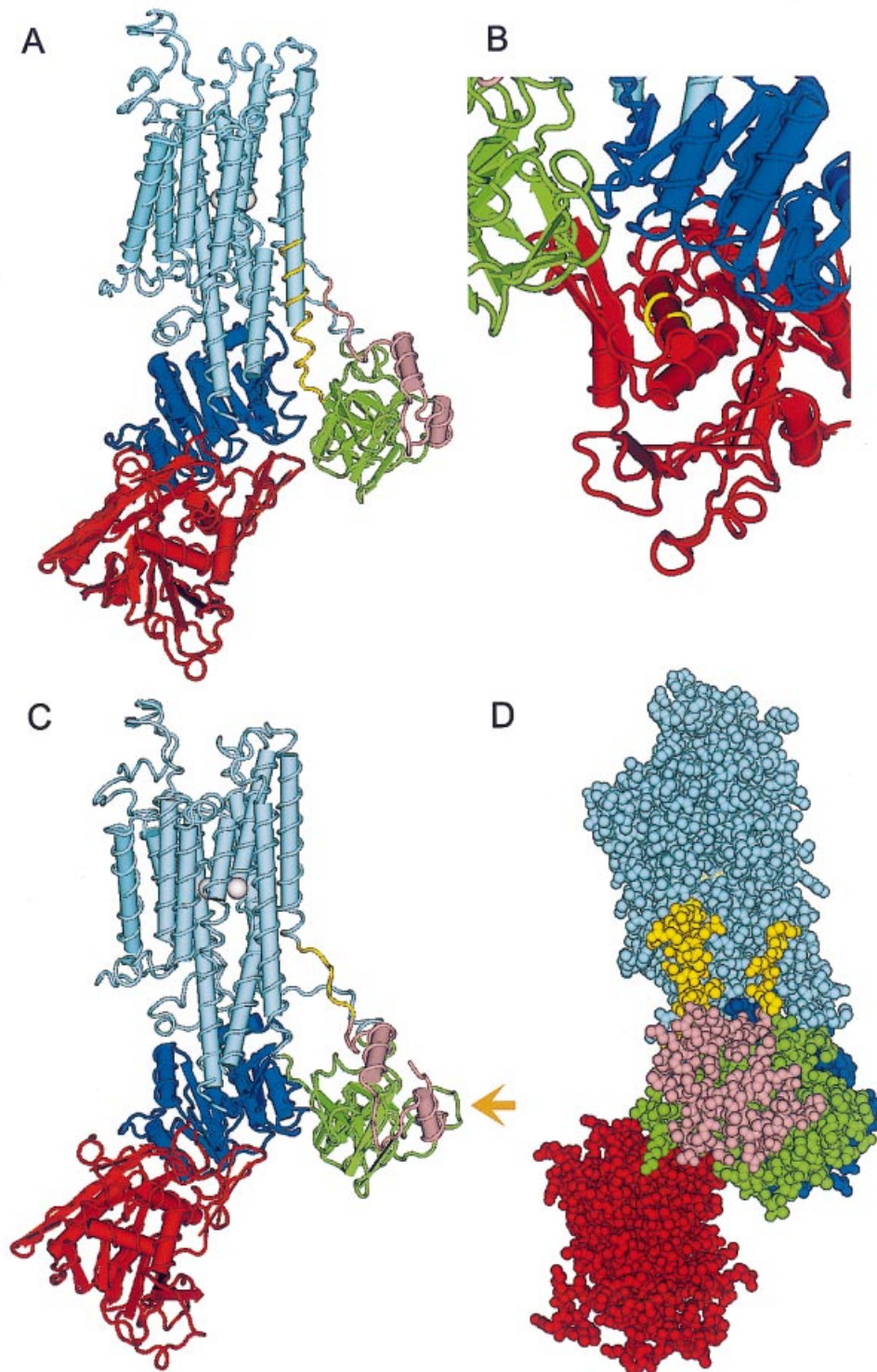


**Figure 13 Protein association sites**

Projected binding sites on Na,K-ATPase for ankyrin (**A** and **B**) and SH3 domain binding proteins (**C**). The high-affinity ankyrin binding site on the end of M2 is very well exposed (**A**). The low-affinity site ALLK (**B**) is completely buried and perhaps not credible unless Na,K-ATPase N domain structure differs here. The SH3 domain protein binding site is well exposed just before M1 (**C**). (**D**) shows in yellow the ankyrin (left) and SH3 (right) sites side-by-side in spacefill format on the extended sequences that link the A domain to the membrane domain. The structure is rotated relative to that in (**A**) and (**C**), and the point of view is indicated by the buff arrow on (**C**).

Phosphoinositide 3-kinase has been proposed to bind to the Na,K-ATPase through its SH3 domain at the high-proline site TPPPTTP, which is on the stretch that links the N-terminal part of the A domain to M1 (Figure 13C). This stretch is highly exposed on the SERCA structure, and, despite the paucity of proline residues in SERCA, the surrounding sequence is otherwise well-conserved. The SH3 domain-containing phosphoinositide 3-kinase is involved in controlling Na,K-ATPase down-regulation by endocytosis [128].

Both the ankyrin site and the SH3-domain-binding site are exceptionally well exposed on adjacent strands (Figure 13D). A quite different specific conformation was predicted for the ankyrin site on the basis of a crystal structure of a fusion protein containing the ankyrin-binding sequence: the sequence was found to form a hairpin structure (a seven-residue loop capping a double  $\beta$  strand) [126]. This has little in common with the SERCA structure, but the A domain is thought to undergo a radical rotation in the course of normal conformation changes [1], necessitating the twisting of both of the exposed strands. Given the probable importance of the flexibility of the A domain connectors, one could speculate that proteins that bind to them might inhibit enzyme activity. On the contrary, ankyrin has been shown to stimulate Na,K-ATPase activity with an effect on a rate-limiting conformation change [129]. The structural features shown here suggest new avenues of investigation.

### BINDING SITE FOR CARDIAC GLYCOSIDES

Cardiac glycosides, including digitalis and ouabain, are the prototypical inhibitors of the Na,K-ATPase subfamily, inhibiting all paralogues to some extent, except the gastric H,K-ATPase. It

has been known since before the discovery of the Na,K-ATPase that cardiac glycosides act from the extracellular surface [130,131]. Ouabain-resistant mutations have led to the identification of 18 amino acids that individually affect the apparent affinity for cardiac glycosides, as detected by ability to survive in the presence of the inhibitor [56,91,132–140]. Figure 14 shows the locations of these residues projected on to the SERCA structure. All but four (three in M4b in the cytoplasmic half after the kink, and one in M7) are close to the extracellular surface. This general conclusion is not new, but the details differ. Certain residues that were predicted to be within the membrane (Cys<sup>104</sup>, Tyr<sup>124</sup>, Thr<sup>797</sup> and Phe<sup>882</sup>) are closer to the surface in the SERCA-based prediction. Phe<sup>863</sup> was predicted to be at the surface at the end of M7, but in the projection it is buried, and Arg<sup>880</sup>, which was predicted to be high on the L7–8 extracellular loop, is instead projected to be just at the end of M7. Any predictions based on homology with M7 should be viewed with caution, since in the Na,K-ATPase it has insertions that could alter the extramembranous exposure of one end or the other, but as mentioned above, the homology is better at the extracellular end than the intracellular end, and so the positions for Phe<sup>863</sup> and Arg<sup>880</sup> shown in Figure 14 may be preferred. Most of the residues conferring resistance to cardiac glycosides are distributed over at least four extracellular loops, L1–2, L3–4, L5–6, and L7–8. The last loop, L9–10, is effectively blocked from access by the vertical bulk of the larger L7–8 loop, but there nonetheless are effects of a residue predicted to be in M10, to the side of the L7–8 loop. The distribution is consistent with solid-state NMR evidence that ouabain lies across the surface [141].

An inhibitor of the gastric H,K-ATPase, SCH 28080, also binds at the extracellular surface. Considerable work has attempted to delineate the site of binding, and in aggregate the evidence supports binding distributed over several extracellular loops, as for ouabain [103,142,143]. Most interesting are the various reports of the inhibition of chimaeras between Na,K-ATPase and H,K-ATPase: in several cases, the chimaeras can be inhibited by both ouabain and SCH28080, or gastric H,K-ATPase acquires the ability to be inhibited by ouabain [144–148]. Even chimaeras with SERCA can show ouabain-sensitivity [149]. The resulting perspective is that binding to the extracellular surface prevents necessary movements of the transmembrane domains relative to one another [138].

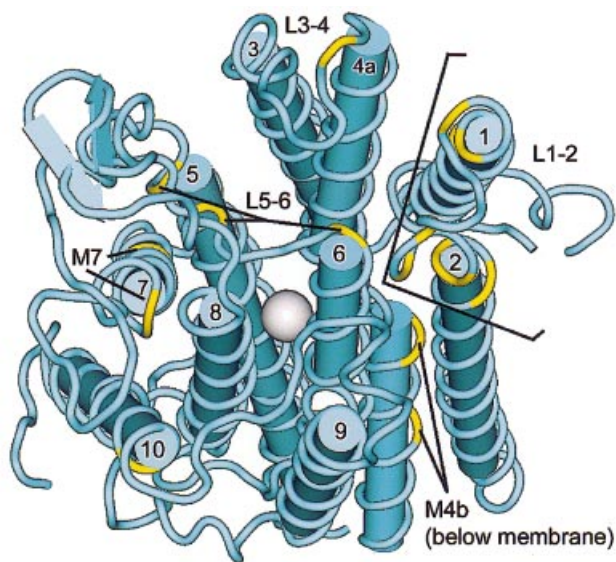


**Figure 14** Ouabain-binding site

The projected locations of residues that affect ouabain binding to Na,K-ATPase are displayed on the SERCA structure. The view is from the extracellular side of the membrane domain, but tilted at a 45° angle to display all of the sites at the same time. Three sites (two in M4b and one in M7) are buried, but all of the rest are close to the surface of the protein. L1–2 has eight sites (sheep numbering), Cys<sup>104</sup>, Tyr<sup>108</sup>, Gln<sup>111</sup>, Glu<sup>116</sup>, Pro<sup>118</sup>, Asp<sup>121</sup>, Asn<sup>122</sup>, and Tyr<sup>124</sup>. L3–4 has one site: Tyr<sup>309</sup>. M4b has three sites: Leu<sup>331</sup>, Ala<sup>332</sup> and Thr<sup>339</sup>. L5–6 has three sites: Phe<sup>783</sup>, Leu<sup>790</sup>, and Thr<sup>794</sup>. M7 has Phe<sup>863</sup>, and L7–8 has Arg<sup>880</sup>. M10 has Phe<sup>882</sup>.

### CONCLUSIONS

The likelihood that the Na,K-ATPase and SERCA Ca<sup>2+</sup>-ATPase have the same fold is very high, considering the 30% identity and 65% similarity in sequence, and the high degree of alignment obtained with gapped-BLAST. Many of the specific examples shown above are consistent with a shared fold, particularly the surface locations of sites of proteolysis; the fact that most insertion/deletion points are at the surface; the locations of accessible cysteine residues at the extracellular surface; and the locations of the sites for binding of other proteins. The biggest discrepancies are in the predicted locations of residues that are known to be cross-linked, but the need for structural perturbation to obtain cross-linking in some cases may be the root cause, or there may be better apposition of the identified regions in another conformation. The other major difference between Ca<sup>2+</sup>-ATPase and Na,K-ATPase is the presence of two additional subunits in the latter: the  $\beta$  subunit in all tissues and the  $\gamma$  subunit in the kidney. These must increase the total number of transmembrane spans from 10 to 12, and they may induce some rearrangement of associated helices from the  $\alpha$  subunit. The

superior alignment of SERCA with Na,K-ATPase compared with PMCA and other members of the gene family suggests a modification of phylogenetic relationships based on structure, to supplement the known evolutionary relationships.

## REFERENCES

- Toyoshima, C., Nakasako, M., Nomura, H. and Ogawa, H. (2000) Crystal structure of the calcium pump of sarcoplasmic reticulum at 2.6 Å resolution. *Nature (London)* **405**, 647–655
- Doyle, D. A., Cabral, R. A., Puetzner, R. A., Koo, A., Gulbis, J. M., Cohen, S. L., Chait, B. T. and MacKinnon, R. J. (1998) The structure of the potassium channel: molecular basis of K<sup>+</sup> conduction and selectivity. *Science* **280**, 69–77
- Ogawa, H., Stokes, D. L., Sasabe, H. and Toyoshima, C. (1998) Structure of the Ca<sup>2+</sup> pump of sarcoplasmic reticulum: a view along the lipid bilayer at 9-Å resolution. *Biophys. J.* **75**, 41–52
- Zhang, P., Toyoshima, C., Yonekura, K., Green, N. M. and Stokes, D. L. (1998) Structure of the calcium pump from sarcoplasmic reticulum at 8-Å resolution. *Nature (London)* **392**, 835–839
- Auer, M., Scarborough, G. A. and Kuhlbrandt, W. (1998) Three-dimensional map of the plasma membrane H<sup>+</sup>-ATPase in the open conformation. *Nature (London)* **392**, 840–843
- Kuhlbrandt, W., Auer, M. and Scarborough, G. A. (1998) Structure of the P-type ATPases. *Curr. Opin. Struct. Biol.* **8**, 510–516
- Scarborough, G. A. (1999) Structure and function of the P-type ATPases. *Curr. Opin. Cell Biol.* **11**, 517–522
- Hebert, H., Xian, Y., Thomsen, K. and Maunsbach, A. B. (2000) Structure of renal Na,K-ATPase as observed by cryo-EM of 2-D crystals. In *Na/K-ATPase and Related ATPases* (Taniguchi, K. and Kaya, S., eds.), pp. 43–48, Elsevier, Amsterdam
- Moller, J. V., Juul, B. and le Maire, M. (1996) Structural organization, ion transport, and energy transduction of P-type ATPases. *Biochim. Biophys. Acta* **1286**, 1–51
- Jorgensen, P. L., Nielsen, J. M., Rasmussen, J. H. and Pedersen, P. A. (1998) Structure–function relationships of E1–E2 transitions and cation binding in Na,K-pump protein. *Biochim. Biophys. Acta* **1365**, 65–70
- Palmgren, M. G. and Axelsen, K. B. (1998) Evolution of P-type ATPases. *Biochim. Biophys. Acta* **1365**, 37–45
- Axelsen, K. B. and Palmgren, M. G. (1998) Evolution of substrate specificities in the P-type ATPase superfamily. *J. Mol. Evol.* **46**, 84–101
- Green, N. M. (1989) ATP-driven cation pumps: alignment of sequences. *Biochem. Soc. Trans.* **17**, 972–974
- Moller, J. V., Juul, B., Maunsbach, A. B., le Maire, M., Menguy, T. and Falson, P. (2000) Topology and plasticity of the membrane bound domains of sarcoplasmic reticulum Ca<sup>2+</sup>-ATPase and Na<sup>+</sup>,K<sup>+</sup>-ATPase. In *Na/K-ATPase and Related ATPases* (Taniguchi, K. and Kaya, S., eds.), pp. 155–162, Elsevier
- Altschul, S. F., Madden, T. L., Schaffer, A. A., Zhang, J., Miller, W. and Lipman, D. J. (1997) Gapped BLAST and PSI-BLAST: a new generation of protein database search programs. *Nucleic Acids Res.* **25**, 3389–3402
- Lee, A. G. and East, J. M. (2001) What the structure of a calcium pump tells us about its mechanism. *Biochem. J.* **356**, 665–683
- MacLennan, D. H. and Green, N. M. (2000) Pumping ions. *Nature (London)* **405**, 633–634
- Lutsenko, S. and Kaplan, J. H. (1995) Organization of P-type ATPases: significance of structural diversity. *Biochemistry* **34**, 15607–15613
- Catty, P., de Kerchove d'Exaerde, A. and Gofeau, A. (1995) The complete inventory of the yeast *Saccharomyces cerevisiae* P-type transport ATPases. *FEBS Lett.* **409**, 325–332
- Halleck, M. S., Pradhan, D., Blackman, C., Berkes, C., Williamson, P. and Schlegel, R. A. (1998) Multiple members of a third subfamily of P-type ATPases identified by genomic sequences and ESTs. *Genome Res.* **8**, 354–361
- Bull, L. N., van Eijk, M. J. T., Pawlikowska, L., DeYoung, J. A., Juijin, J. A., Liao, M., Klomp, L. W. J., Lomri, N., Berger, R., Scharnschmidt, B. F. et al. (1998) A gene encoding a P-type ATPase mutated in two forms of hereditary cholestasis. *Nat. Genet.* **18**, 219–224
- Penniston, J. T. and Enyedi, A. (1998) Modulation of the plasma membrane Ca<sup>2+</sup> pump. *J. Membr. Biol.* **165**, 101–109
- Strehler, E. E. and Zacharias, D. A. (2001) Role of alternative splicing in generating isoform diversity among plasma membrane calcium pumps. *Physiol. Rev.* **81**, 21–50
- Tang, X., Halleck, M. S., Schlegel, R. A. and Williamson, P. (1996) A subfamily of P-type ATPases with aminophospholipid transporting activity. *Science* **272**, 1495–1497
- Siegmund, A., Grant, A., Angeletti, C., Malone, L., Nichols, J. W. and Rudolph, H. K. (1998) Loss of Drs2p does not abolish transfer of fluorescence-labeled phospholipids across the plasma membrane of *Saccharomyces cerevisiae*. *J. Biol. Chem.* **273**, 34399–34405
- Lutsenko, S., Daoud, S. and Kaplan, J. H. (1997) Identification of two conformationally sensitive cysteine residues at the extracellular surface of the Na,K-ATPase  $\alpha$ -subunit. *J. Biol. Chem.* **272**, 5249–5255
- Bar Shimon, M., Goldshleger, R. and Karlish, S. J. D. (1998) Specific Cu<sup>2+</sup>-catalyzed oxidative cleavage of Na,K-ATPase at the extracellular surface. *J. Biol. Chem.* **273**, 34190–34195
- Hu, Y.-K. and Kaplan, J. H. (2000) Site-directed chemical labeling of extracellular loops in a membrane protein. The topology of the Na,K-ATPase  $\alpha$ -subunit. *J. Biol. Chem.* **275**, 19185–19191
- Jorgensen, P. L. (1992) Na,K-ATPase, structure and transport mechanism. In *Molecular Aspects of Transport Proteins* (De Pont, J. J. H. M., ed.), Pp. 1–26, Elsevier Science Publishers, Amsterdam and New York
- Jorgensen, P. L. and Andersen, J. P. (1988) Structural basis for E1–E2 conformational transitions in Na,K-pump and Ca-pump proteins. *J. Membr. Biol.* **103**, 95–120
- Felsenfeld, D. P. and Sweadner, K. J. (1988) Fine specificity mapping and topography of an isozyme-specific epitope of the Na,K-ATPase catalytic subunit. *J. Biol. Chem.* **263**, 10932–10942
- Sato, H., Nakao, T., Nagai, F., Kano, I., Nakagawa, A., Ushiyama, K., Urayama, O., Hara, Y. and Nakao, M. (1989) A monoclonal antibody against horse kidney (Na<sup>+</sup> + K<sup>+</sup>)-ATPase inhibits sodium pump and E2K to E1 conversion of (Na<sup>+</sup> + K<sup>+</sup>)-ATPase from outside of the cell membrane. *Biochim. Biophys. Acta* **994**, 104–113
- Arystarkhova, E., Gasparian, M., Modyanov, N. N. and Sweadner, K. J. (1992) Na,K-ATPase extracellular surface probed with a monoclonal antibody that enhances ouabain binding. *J. Biol. Chem.* **267**, 13694–13701
- Sweadner, K. J. and Arystarkhova, E. (1992) Constraints on models for the folding of the Na,K-ATPase. *Ann. N. Y. Acad. Sci. U.S.A.* **671**, 217–227
- Smolka, A. and Swiger, K. M. (1992) Site-directed antibodies as topographical probes of the gastric H,K-ATPase alpha-subunit. *Biochim. Biophys. Acta* **1108**, 75–85
- Ning, G., Maunsbach, A. B., Lee, Y. J. and Moller, J. V. (1993) Topology of Na,K-ATPase alpha subunit epitopes analyzed with oligopeptide-specific antibodies and double-labeling immunoelectron microscopy. *FEBS Lett.* **336**, 521–524
- Scully, R. R., Pressley, T. A. and O'Neil, R. G. (1993) A site-directed antibody recognizes a component of the ouabain-binding domain of the alpha 1 subunit of rat Na<sup>+</sup>,K<sup>+</sup>-ATPase. *Biochem. Cell Biol.* **71**, 538–543
- Mercier, F., Bayle, D., Besancon, M., Joys, T., Shin, J. M., Lewin, M. J. M., Prinz, C., Reuben, M. A., Soumarmon, A., Wong, H., Walsh, J. H. and Sachs, G. (1993) Antibody epitope mapping of the gastric H<sup>+</sup>/K<sup>+</sup>-ATPase. *Biochim. Biophys. Acta* **1149**, 151–165
- Mohraz, M., Arystarkhova, E. and Sweadner, K. J. (1994) Immunoelectronmicroscopy of epitopes on Na,K-ATPase catalytic subunit. Implications for the transmembrane organization of the C-terminal domain. *J. Biol. Chem.* **269**, 2929–2936
- Arystarkhova, E. and Sweadner, K. J. (1996) Isoform-specific monoclonal antibodies to Na,K-ATPase  $\alpha$  subunits: evidence for a tissue-specific post-translational modification of the  $\alpha$  subunit. *J. Biol. Chem.* **271**, 23407–23417
- Smolka, A., Larsen, K. A. and Hammond, C. E. (2000) Location of a cytoplasmic epitope for monoclonal antibody HK 12.18 on H,K-ATPase  $\alpha$  subunit. *Biochem. Biophys. Res. Commun.* **273**, 942–947
- Donnet, C., Arystarkhova, E. and Sweadner, K. J. (2001) Thermal denaturation of the Na,K-ATPase provides evidence for  $\alpha$ - $\alpha$  oligomeric interaction and  $\gamma$  subunit association with the C-terminal domain. *J. Biol. Chem.* **276**, 7357–7365
- Ovchinnikov, Y., Luneva, N. M., Arystarkhova, E. A., Gevondyan, N. M., Arzamazova, N. M., Kozhich, A. T., Nesmeyanov, V. A. and Modyanov, N. N. (1988) Topology of Na<sup>+</sup>,K<sup>+</sup>-ATPase. Identification of the extra- and intracellular hydrophilic loops of the catalytic subunit by specific antibodies. *FEBS Lett.* **227**, 230–234
- Lutsenko, S., Anderko, R. and Kaplan, J. H. (1995) Membrane disposition of the M5–M6 hairpin of Na<sup>+</sup>,K<sup>+</sup>-ATPase  $\alpha$  subunit is ligand-dependent. *Proc. Natl. Acad. Sci. U.S.A.* **92**, 7936–7940
- Shainskaya, A., Nesaty, V. and Karlish, S. J. D. (1998) Interactions between fragments of trypsinized Na,K-ATPase detected by thermal inactivation of Rb<sup>+</sup> occlusion and dissociation of the M5/M6 fragment. *J. Biol. Chem.* **273**, 7311–7319
- Gatto, C., Lutsenko, S., Shin, J. M., Sachs, G. and Kaplan, J. G. (1999) Stabilization of the H,K-ATPase M5M6 membrane hairpin by K<sup>+</sup> ions. Mechanistic significance for P-2-type ATPases. *J. Biol. Chem.* **274**, 13737–13740
- Canfield, V. A. and Levenson, R. (1993) Transmembrane organization of the Na,K-ATPase determined by epitope addition. *Biochemistry* **32**, 13782–13786
- Yoon, K. L. and Guidotti, G. (1994) Studies on the membrane topology of the (Na,K)-ATPase. *J. Biol. Chem.* **269**, 28249–28258

- 49 Canfield, V. A., Norbeck, L. and Levenson, R. (1996) Localization of cytoplasmic and extracellular domains of Na,K-ATPase by epitope tag insertion. *Biochemistry* **35**, 14165–14172
- 50 Lee, K. and Guidotti, G. (1998) Residue Leu973 of the rat  $\alpha$ 1 subunit of the Na,K-ATPase is located on the cytoplasmic side of the plasma membrane. *Biochem. Biophys. Res. Commun.* **251**, 693–698
- 51 Anderberg, S. J. (1995) Topological disposition of lysine 943 in native Na<sup>+</sup>/K<sup>+</sup>-transporting ATPase. *Biochemistry* **34**, 9508–9516
- 52 Smolka, A. J., Larsen, K. A., Schweinfest, C. W. and Hammond, C. E. (1999) H,K-ATPase  $\alpha$ -subunit C-terminal membrane topology: epitope tags in the insect cell expression system. *Biochem. J.* **340**, 601–611
- 53 Fiedler, B. and Scheiner-Bobis, G. (1996) Transmembrane topology of  $\alpha$ - and  $\beta$ -subunits of Na<sup>+</sup>,K<sup>+</sup>-ATPase derived from  $\beta$ -galactosidase fusion proteins expressed in yeast. *J. Biol. Chem.* **271**, 29312–29320
- 54 Beguin, P., Hasler, U., Staub, O. and Geering, K. (2000) Endoplasmic reticulum quality control of oligomeric membrane proteins: topogenic determinants involved in the degradation of the unassembled Na,K-ATPase  $\alpha$  subunit and in its stabilization by  $\beta$  subunit assembly. *Mol. Biol. Cell* **11**, 1657–1672
- 55 Beguin, P., Hasler, U., Beggah, A., Horisberger, J. D. and Geering, K. (1998) Membrane integration of Na,K-ATPase alpha-subunits and beta subunit assembly. *J. Biol. Chem.* **273**, 24921–24931
- 56 Schneider, H. and Scheiner-Bobis, G. (1997) Involvement of the M7/M8 extracellular loop of the sodium pump  $\alpha$  subunit in ion transport. Structural and functional homology to P-loops of ion channels. *J. Biol. Chem.* **272**, 16158–16165
- 57 Moller, J. V., Ning, G., Maunsbach, A. B., Fujimoto, K., Asai, K., Juul, B., Lee, Y.-J., Gomez de Gracia, A., Falson, P. and le Maire, M. (1997) Probing of the membrane topology of sarcoplasmic reticulum Ca<sup>2+</sup>-ATPase with sequence-specific antibodies. *J. Biol. Chem.* **272**, 29015–29032
- 58 Colonna, T. E., Huynh, L. and Fambrough, D. M. (1997) Subunit interactions in the Na,K-ATPase explored with the yeast two-hybrid system. *J. Biol. Chem.* **272**, 12366–12372
- 59 Or, E., Goldshleger, R., Shainskaya, A. and Karlish, S. J. D. (1998) Specific cross-links between fragments of proteolyzed Na,K-ATPase induced by  $\alpha$ -phthalaldehyde. *Biochemistry* **37**, 8197–8207
- 60 Melle-Milovanovic, D., Milovanovic, M., Nagpal, S., Sachs, G. and Shin, J. M. (1998) Regions of association between the alpha and the beta subunit of the gastric H,K-ATPase. *J. Biol. Chem.* **273**, 11075–11081
- 61 Capasso, J. M., Hoving, S., Tal, D. M., Goldshleger, R. and Karlish, S. J. D. (1992) Extensive digestion of Na<sup>+</sup>,K<sup>+</sup>-ATPase by specific and nonspecific proteases with preservation of cation occlusion sites. *J. Biol. Chem.* **267**, 1150–1158
- 62 Shin, J. M., Besancon, M., Simon, A. and Sachs, G. (1993) The site of action of pantoprazole in the gastric H<sup>+</sup>/K<sup>+</sup>-ATPase. *Biochim. Biophys. Acta* **1148**, 223–233
- 63 Lutsenko, S. and Kaplan, J. H. (1994) Molecular events in close proximity to the membrane associated with the binding of ligands to the Na,K-ATPase. *J. Biol. Chem.* **269**, 4555–4564
- 64 Shin, J. M., Kajimura, M., Arguello, J. M., Kaplan, J. H. and Sachs, G. (1994) Biochemical identification of transmembrane segments of the Ca<sup>2+</sup>-ATPase of sarcoplasmic reticulum. *J. Biol. Chem.* **269**, 22533–22537
- 65 Juul, B., Turc, H., Durand, M. L., Gomez de Gracia, A., Denoroy, L., Moller, J. V., Champeil, P. and le Maire, M. (1995) Do transmembrane segments in proteolyzed sarcoplasmic reticulum Ca<sup>2+</sup>-ATPase retain their functional Ca<sup>2+</sup> binding properties after removal of cytoplasmic fragments by proteinase K? *J. Biol. Chem.* **270**, 20123–20134
- 66 Raussens, V., Ruysschaert, J. M. and Goormaghtigh, E. (1997) Fourier transform infrared spectroscopy study of the secondary structure of the gastric H<sup>+</sup>,K<sup>+</sup>-ATPase and of its membrane-associated proteolytic peptides. *J. Biol. Chem.* **272**, 262–270
- 67 Munson, K. B., Gutierrez, C., Balaji, V. N., Ramnarayan, K. and Sachs, G. (1991) Identification of an extracytoplasmic region of H<sup>+</sup>,K<sup>+</sup>-ATPase labeled by a K<sup>+</sup>-competitive photoaffinity inhibitor. *J. Biol. Chem.* **266**, 18976–18988
- 68 Shainskaya, A. and Karlish, S. J. D. (1994) Evidence that the cation occlusion domain of Na/K-ATPase consists of a complex of membrane-spanning segments. *J. Biol. Chem.* **269**, 10780–10789
- 69 Shainskaya, A. and Karlish, S. J. D. (1996) Chymotryptic digestion of the cytoplasmic domain of the beta subunit of Na/K-ATPase alters kinetics of occlusion of Rb<sup>+</sup> ions. *J. Biol. Chem.* **271**, 10309–10316
- 70 Ivanov, A., Askari, A. and Modyanov, N. N. (1997) Structural analysis of the products of chymotryptic cleavage of the E1 form of Na,K-ATPase alpha-subunit: identification of the N-terminal fragments containing the transmembrane H1–H2 domain. *FEBS Lett.* **420**, 107–111
- 71 Karlish, S. J. D., Goldshleger, R. and Jorgensen, P. L. (1993) Location of Asn 831 of the alpha chain of Na,K-ATPase at the cytoplasmic surface: implication for topological models. *J. Biol. Chem.* **268**, 3471–3478
- 72 Besancon, M., Shin, J. M., Mercier, F., Munson, K., Miller, M., Hersey, S. and Sachs, G. (1993) Membrane topology and omeprazole labeling of the gastric H<sup>+</sup>,K<sup>+</sup>-adenosinetriphosphatase. *Biochemistry* **32**, 2345–2355
- 73 Tai, M. M., Im, W. B., Davis, J. P., Blakeman, D. P., Zurcher-Neely, H. A. and Heinrikson, R. L. (1989) Evidence for the presence of a carbohydrate moiety in fluorescein isothiocyanate labeled fragments of rat gastric (H<sup>+</sup>-K<sup>+</sup>)-ATPase. *Biochemistry* **28**, 3183–3187
- 74 Van Uem, T. J. F., Swarts, H. G. P. and De Pont, J. J. H. H. M. (1991) Determination of the epitope for the inhibitory monoclonal antibody 5-B6 on the catalytic subunit of gastric Mg<sup>2+</sup>-dependent H<sup>+</sup>-transporting and K<sup>+</sup>-stimulated ATPase. *Biochem. J.* **280**, 243–248
- 75 Tran, C. M., Huston, E. E. and Farley, R. A. (1994) Photochemical labeling and inhibition of Na,K-ATPase by 2-azido-ATP. Identification of an amino acid located within the ATP binding site. *J. Biol. Chem.* **269**, 6558–6565
- 76 Champeil, P., Menguy, T., Soulie, S., Juul, B., Gomez de Gracia, A., Rusconi, F., Falson, P., Denoroy, L., Henao, F., le Maire, M. and Moller, J. V. (1998) Characterization of a protease-resistant domain of the cytosolic portion of sarcoplasmic reticulum Ca<sup>2+</sup>-ATPase. *J. Biol. Chem.* **273**, 6619–6631
- 77 Gatto, C., Wang, A. X. and Kaplan, J. H. (1998) The M4M5 cytoplasmic loop of the Na,K-ATPase, overexpressed in *Escherichia coli*, binds nucleoside triphosphates with the same selectivity as the intact native protein. *J. Biol. Chem.* **273**, 10578–10585
- 78 Moutin, M. J., Rapin, C., Miras, R., Vincon, M., Dupont, Y. and McIntosh, D. B. (1998) Autonomous folding of the recombinant large cytoplasmic loop of sarcoplasmic reticulum Ca<sup>2+</sup>-ATPase probed by affinity labeling and trypsin digestion. *Eur. J. Biochem.* **251**, 682–690
- 79 Tran, C. M. and Farley, R. A. (1999) Catalytic activity of an isolated domain of Na,K-ATPase expressed in *Escherichia coli*. *Biophys. J.* **77**, 258–266
- 80 Jorgensen, P. L. and Collins, J. H. (1986) Tryptic and chymotryptic cleavage sites in sequence of alpha-subunit of (Na<sup>+</sup> + K<sup>+</sup>)-ATPase from outer medulla of mammalian kidney. *Biochim. Biophys. Acta* **860**, 570–576
- 81 Karlish, S. J. D., Goldshleger, R. and Stein, W. D. (1990) A 19-kDa C-terminal tryptic fragment of the alpha chain of Na/K-ATPase is essential for occlusion and transport of cations. *Proc. Natl. Acad. Sci. U.S.A.* **87**, 4566–4570
- 82 Arystarkhova, E., Gibbons, D. L. and Sweadner, K. J. (1995) Topology of the Na,K-ATPase: evidence for externalization of a labile transmembrane structure during heating. *J. Biol. Chem.* **270**, 8785–8796
- 83 Goldshleger, R., Tal, D. M. and Karlish, S. J. D. (1995) Topology of the  $\alpha$ -subunit of Na,K-ATPase based on proteolysis. Lability of the topological organization. *Biochemistry* **34**, 8668–8679
- 84 Liu, L. and Askari, A. (1997) Evidence for the existence of two ATP-sensitive Rb<sup>+</sup> occlusion pockets within the transmembrane domains of Na<sup>+</sup>/K<sup>+</sup>-ATPase. *J. Biol. Chem.* **272**, 14380–14386
- 85 Simmerman, H. K. B. and Jones, L. R. (1998) Phospholamban: protein structure, mechanism of action, and role in cardiac function. *Physiol. Rev.* **78**, 921–947
- 86 Asahi, M., Kimura, Y., Kurzydowski, K. and Tada, M. (1999) Transmembrane helix M6 in sarco(endo)plasmic reticulum Ca<sup>2+</sup>-ATPase forms a functional interaction site with phospholamban. *J. Biol. Chem.* **274**, 32855–32862
- 87 James, P., Inui, M., Tada, M., Chiesi, M. and Carafoli, E. (1989) Nature and site of phospholamban regulation of the Ca<sup>2+</sup> pump of sarcoplasmic reticulum pump of sarcoplasmic reticulum. *Nature (London)* **342**, 90–92
- 88 Toyofuku, T., Kurzydowski, K., Tada, M. and MacLennan, D. H. (1994) Amino acids Lys-Asp-Lys-Pro-Val402 in the Ca<sup>2+</sup>-ATPase of cardiac sarcoplasmic reticulum are critical for functional association with phospholamban. *J. Biol. Chem.* **269**, 22929–22932
- 89 Shi, H. G., Mikhaylova, L., Zichitella, A. E. and Arguello, J. M. (2000) Functional role of cysteine residues in the (Na,K)-ATPase  $\alpha$  subunit. *Biochim. Biophys. Acta* **1464**, 177–187
- 90 Hu, Y.-K., Eisses, J. F. and Kaplan, J. H. (2000) Expression of an active Na-K-ATPase with an  $\alpha$ -subunit lacking all twenty-three native cysteine residues. *J. Biol. Chem.* **275**, 30734–30739
- 91 Canessa, C. M., Horisberger, J.-D., Louvard, D. and Rossier, B. C. (1992) Mutations of a cysteine in the first transmembrane segment of Na,K-ATPase alpha subunit confers ouabain resistance. *EMBO J.* **11**, 1681–1687
- 92 Antolovic, R., Linder, D., Hahnen, J. and Schoner, W. (1995) Affinity labeling of a sulfhydryl group in the cardiac glycoside receptor site of Na<sup>+</sup>/K<sup>+</sup>-ATPase by N-hydroxysuccinimidyl derivatives of digoxigenin. *Eur. J. Biochem.* **227**, 61–67
- 93 Antolovic, R., Schoner, W., Geering, K., Canessa, C., Rossier, B. C. and Horisberger, J.-D. (1995) Labeling of a cysteine in the cardiotonic glycoside binding site by the steroid derivative HDMA. *FEBS Lett.* **368**, 169–172
- 94 Wang, X. and Horisberger, J.-D. (1996) Mercury binding site on Na<sup>+</sup>/K<sup>+</sup>-ATPase: a cysteine in the first transmembrane segment. *Mol. Pharmacol.* **50**, 687–691
- 95 Zichitella, A. E., Shi, H. G. and Arguello, J. M. (2000) Reactivity of cysteines in the transmembrane region of the Na,K-ATPase  $\alpha$  subunit probed with Hg<sup>2+</sup>. *J. Membr. Biol.* **177**, 187–197

- 96 Repke, K. R. H., Sweadner, K. J., Weiland, J., Megges, R. and Schon, R. (1996) In search of ideal inotropic steroids: recent progress. *Prog. Drug Res.* **47**, 9–52
- 97 Taniguchi, K., Tosa, H., Suzuki, K. and Kamo, Y. (1988) Microenvironment of two different extrinsic fluorescence probes in Na<sup>+</sup>,K<sup>+</sup>-ATPase changes out of phase during sequential appearance of reaction intermediates. *J. Biol. Chem.* **263**, 12943–12947
- 98 Taniguchi, K. and Mardh, S. (1993) Reversible changes in the fluorescence energy transfer accompanying formation of reaction intermediates in probe-labeled Na<sup>+</sup>,K<sup>+</sup>-ATPase. *J. Biol. Chem.* **268**, 15588–15594
- 99 Wang, S.-G. and Farley, R. A. (1998) Valine 904, tyrosine 898, and cysteine 908 in Na,K-ATPase  $\alpha$ -subunits are important for assembly with  $\beta$ -subunits. *J. Biol. Chem.* **273**, 29400–29405
- 100 Guennoun, S. and Horisberger, J.-D. (2000) Structure of the 5th transmembrane segment of the Na,K-ATPase  $\alpha$  subunit: a cysteine-scanning mutagenesis study. *FEBS Lett.* **482**, 144–148
- 101 Munson, K., Lambrecht, N., Shin, J. M. and Sachs, G. (2000) Analysis of the membrane domain of the gastric H<sup>+</sup>/K<sup>+</sup>-ATPase. *J. Exp. Biol.* **203**, 161–170
- 102 Besançon, M., Simon, A., Sachs, G. and Shin, J. M. (1997) Sites of reaction of the gastric H,K-ATPase with extracytoplasmic thiol reagents. *J. Biol. Chem.* **272**, 22438–22446
- 103 Lambrecht, N., Corbett, Z., Bayle, D., Karlish, S. J. D. and Sachs, G. (1998) Identification of the site of inhibition by omeprazole of an alpha-beta fusion protein of the H,K-ATPase using site-directed mutagenesis. *J. Biol. Chem.* **273**, 13719–13728
- 104 Rice, W. J., Green, N. M. and MacLennan, D. H. (1997) Site-directed disulfide mapping of helices M4 and M6 in the Ca<sup>2+</sup> binding domain of SERCA1a, the Ca<sup>2+</sup> ATPase of fast twitch skeletal muscle sarcoplasmic reticulum. *J. Biol. Chem.* **272**, 31412–31419
- 105 McIntosh, D. B. (1992) Glutaraldehyde cross-links Lys-492 and Arg-678 at the active site of sarcoplasmic reticulum Ca<sup>2+</sup>-ATPase. *J. Biol. Chem.* **267**, 22328–22335
- 106 Ross, D. C. and McIntosh, D. B. (1987) Intramolecular cross-linking at the active site of the Ca<sup>2+</sup>-ATPase of sarcoplasmic reticulum. High and low affinity nucleotide binding and evidence of active site closure in E2-P. *J. Biol. Chem.* **262**, 12977–12983
- 107 Huang, W.-H. and Askari, A. (1979) (Na<sup>+</sup> + K<sup>+</sup>)-ATPase: effects of detergents on the cross-linking of subunits in the presence of Cu<sup>2+</sup> and *o*-phenanthroline. *Biochim. Biophys. Acta* **578**, 547–552
- 108 Periyasamy, S. M., Huang, W.-H. and Askari, A. (1983) Subunit associations of (Na<sup>+</sup> + K<sup>+</sup>)-dependent adenosine triphosphatase. Chemical cross-linking studies. *J. Biol. Chem.* **258**, 9878–9885
- 109 Sarvazyan, N. A., Modyanov, N. N. and Askari, A. (1995) Intersubunit and intrasubunit contact regions of Na<sup>+</sup>/K<sup>+</sup>-ATPase revealed by controlled proteolysis and chemical cross-linking. *J. Biol. Chem.* **270**, 26528–26532
- 110 Or, E., Goldshleger, R. and Karlish, S. J. D. (1999) Characterization of disulfide cross-links between fragments of proteolyzed Na,K-ATPase. *J. Biol. Chem.* **274**, 2802–2809
- 111 Sarvazyan, N. A., Ivanov, A., Modyanov, N. N. and Askari, A. (1997) Ligand-sensitive interactions among the transmembrane helices of Na<sup>+</sup>/K<sup>+</sup>-ATPase. *J. Biol. Chem.* **272**, 7855–7858
- 112 Ivanov, A., Zhao, H. and Modyanov, N. N. (2000) Packing of the transmembrane helices of Na,K-ATPase: direct contact between  $\beta$ -subunit and H8 segment of  $\alpha$ -subunit revealed by oxidative cross-linking. *Biochemistry* **39**, 9778–9785
- 113 Gevondyan, N. M., Gavrielyeva, E. E., Gevondyan, V. S., Grinberg, A. V. and Modyanov, N. N. (1995) Analysis of disulfide-containing fragments of Na<sup>+</sup>,K<sup>+</sup>-ATPase. III. Amino acid sequence of cysteinyl peptides. Location of disulfide bonds of the  $\alpha$ -subunit. *Membr. Cell Biol.* **9**, 19–26
- 114 Lane, L. K. (1993) Functional expression of rat alpha 1 Na,K-ATPase containing substitutions for cysteines 454, 458, 513, and 551. *Biochem. Mol. Biol. Int.* **31**, 817–822
- 115 Shainskaya, A., Schneeberger, A., Apell, H. J. and Karlish, S. J. D. (2000) Entrance port for Na<sup>+</sup> and K<sup>+</sup> ions on Na<sup>+</sup>,K<sup>+</sup>-ATPase in the cytoplasmic loop between trans-membrane segments M6 and M7 of the  $\alpha$  subunit. *J. Biol. Chem.* **275**, 2019–2028
- 116 Zhang, Z., Lewis, D., Strock, C., Inesi, G., Nakasako, M., Nomura, H. and Toyoshima, C. (2000) Detailed characterization of the cooperative mechanism of Ca<sup>2+</sup> binding and catalytic activation in the Ca<sup>2+</sup> transport (SERCA) ATPase. *Biochemistry* **39**, 8758–8767
- 117 Goldshleger, R. and Karlish, S. J. D. (1997) Fe-catalyzed cleavage of the alpha subunit of Na,K-ATPase: evidence for conformation-sensitive interactions between cytoplasmic domains. *Proc. Natl. Acad. Sci. U.S.A.* **94**, 9596–9601
- 118 Goldshleger, R. and Karlish, S. J. D. (1999) The energy transduction mechanism of Na,K-ATPase studied with iron-catalyzed oxidative cleavage. *J. Biol. Chem.* **274**, 16213–16221
- 119 Kasho, V. N., Stengelin, M., Smirnova, I. N. and Faller, L. D. (1997) A proposal for the Mg<sup>2+</sup> binding site of P-type ion motive ATPases and the mechanism of phosphoryl group transfer. *Biochemistry* **36**, 8045–8052
- 120 Farley, R. A., Heart, E., Kabalin, M., Putnam, D., Wang, K., Kasho, V. N. and Faller, L. D. (1997) Site-directed mutagenesis of the sodium pump: analysis of mutations to amino acids in the proposed nucleotide binding site by stable oxygen isotope exchange. *Biochemistry* **36**, 941–951
- 121 Pedersen, P. A., Jorgensen, J. R. and Jorgensen, P. L. (2000) Importance of conserved  $\alpha$ -subunit segment 709GDGVND for Mg<sup>2+</sup> binding, phosphorylation, and energy transduction in Na,K-ATPase. *J. Biol. Chem.* **275**, 37588–37595
- 122 Patchornik, G., Goldshleger, R. and Karlish, S. J. D. (2000) The complex ATP-Fe<sup>2+</sup> serves as a specific affinity cleavage reagent in ATP-Mg<sup>2+</sup> sites of Na,K-ATPase: altered ligation of Fe<sup>2+</sup> (Mg<sup>2+</sup>) ions accompanies the E1P–E2P conformational change. *Proc. Natl. Acad. Sci. U.S.A.* **97**, 11954–11959
- 123 Goldshleger, R., Patchornik, G., Bar Shimon, M., Tal, D. M., Post, R. L. and Karlish, S. J. D. (2001) Structural organization and the energy transduction mechanism of Na<sup>+</sup>,K<sup>+</sup>-ATPase studied with transition metal-catalyzed oxidative cleavage. *J. Bioenerg. Biomembr.*, in the press
- 124 Sweadner, K. J. and Feschenko, M. S. (2001) Predicted location and limited accessibility of the protein kinase A phosphorylation site on Na,K-ATPase. *Am. J. Physiol.* **280**, C1017–C1026
- 125 Devarajan, P., Scaramuzzino, D. A. and Morrow, J. S. (1994) Ankyrin binds to two distinct cytoplasmic domains of Na,K-ATPase alpha subunit. *Proc. Natl. Acad. Sci. U.S.A.* **91**, 2965–2969
- 126 Zhang, A., Devarajan, P., Dorfman, A. L. and Morrow, J. S. (1998) Structure of the ankyrin-binding domain of alpha-Na,K-ATPase. *J. Biol. Chem.* **273**, 18681–18684
- 127 Jordan, C., Puschel, B., Koob, R. and Drenckhahn, D. (1995) Identification of a binding motif for ankyrin on the  $\alpha$ -subunit of Na<sup>+</sup>,K<sup>+</sup>-ATPase. *J. Biol. Chem.* **270**, 29971–29975
- 128 Yudowski, G. A., Efendiev, R., Pedemonte, C. H., Katz, A. I., Berggren, P. O. and Bertorello, A. (2000) Phosphoinositide-3 kinase binds to a proline-rich motif in the Na<sup>+</sup>,K<sup>+</sup>-ATPase  $\alpha$  subunit and regulates its trafficking. *Proc. Natl. Acad. Sci. U.S.A.* **97**, 6556–6561
- 129 Ferrandi, M., Salardi, S., Tripodi, G., Barassi, P., Rivera, R., Manuta, P., Goldshleger, R., Ferrari, P., Bianchi, G. and Karlish, S. J. D. (1999) Evidence for an interaction between adducin and Na<sup>+</sup>-K<sup>+</sup>-ATPase: relation to genetic hypertension. *Am. J. Physiol.* **277**, H1338–H1349
- 130 Hodgkin, A. L. and Keynes, R. D. (1955) Active transport of cations in giant axons from *Sepia* and *Loligo*. *J. Physiol. (London)* **128**, 28–60
- 131 Glynn, I. M. (1956) Sodium and potassium movements in human red cells. *J. Physiol. (London)* **134**, 278–310
- 132 Price, E. M. and Lingrel, J. B. (1988) Structure–function relationships in the Na,K-ATPase alpha subunit: site-directed mutagenesis of glutamine-111 to arginine and asparagine-122 to aspartic acid generates a ouabain-resistant enzyme. *Biochemistry* **27**, 8400–8408
- 133 Price, E. M., Rice, D. A. and Lingrel, J. B. (1989) Site-directed mutagenesis of a conserved, extracellular aspartic acid residue affects the ouabain sensitivity of sheep Na,K-ATPase. *J. Biol. Chem.* **264**, 21902–21906
- 134 Canessa, C. M., Horisberger, J. D. and Rossier, B. C. (1993) Mutation of a tyrosine in the H3–H4 ectodomain of Na,K-ATPase  $\alpha$  subunit confers ouabain resistance. *J. Biol. Chem.* **268**, 17722–17726
- 135 Schultheis, P. J. and Lingrel, J. B. (1993) Substitution of transmembrane residues with hydrogen-bonding potential in the  $\alpha$  subunit of Na,K-ATPase reveals alterations in ouabain sensitivity. *Biochemistry* **32**, 544–550
- 136 Schultheis, P. J., Wallick, E. T. and Lingrel, J. B. (1993) Kinetic analysis of ouabain binding to native and mutated forms of Na,K-ATPase and identification of a new region involved in cardiac glycoside interactions. *J. Biol. Chem.* **268**, 22686–22694
- 137 Burns, E. L. and Price, E. M. (1993) Random mutagenesis of the sheep Na,K-ATPase  $\alpha$ -1 subunit generates a novel T979N mutation that results in a ouabain-resistant enzyme. *J. Biol. Chem.* **268**, 25632–25635
- 138 Palasis, M., Kuntzweiler, T. A., Arguello, J. M. and Lingrel, J. B. (1996) Ouabain interactions with the H5–H6 hairpin of the Na,K-ATPase reveal a possible inhibition mechanism via the cation binding domain. *J. Biol. Chem.* **271**, 14176–14182
- 139 Burns, E. L., Nicholas, R. A. and Price, E. M. (1996) Random mutagenesis of the sheep Na,K-ATPase  $\alpha$ 1 subunit generating the ouabain-resistant mutant L793P. *J. Biol. Chem.* **271**, 15879–15883
- 140 Croyle, M. L., Woo, A. L. and Lingrel, J. B. (1997) Extensive random mutagenesis analysis of the Na,K-ATPase alpha subunit identifies known and previously unidentified amino acid residues that alter ouabain sensitivity. Implications for ouabain binding. *Eur. J. Biochem.* **248**, 488–495
- 141 Middleton, D. A., Rankin, S., Esmann, M. and Watts, A. (2000) Structural insights into the binding of cardiac glycosides to the digitalis receptor revealed by solid-state NMR. *Proc. Natl. Acad. Sci. U.S.A.* **97**, 13602–13607

- 142 Swarts, H. G. P., Hermsen, H. P. H., Koenderink, J. B., Willems, P. H. G. M. and De Pont, J. J. H. M. (1999) Conformation-dependent inhibition of gastric H<sup>+</sup>,K<sup>+</sup>-ATPase by SCH28080 demonstrated by mutagenesis of glutamic acid 820. *J. Pharmacol. Exp. Ther.* **55**, 541–547
- 143 Lambrecht, N., Munson, K., Vagin, O. and Sachs, G. (2000) Comparison of covalent with reversible inhibitor binding sites of the gastric H,K-ATPase by site-directed mutagenesis. *J. Biol. Chem.* **275**, 4041–4048
- 144 Blostein, R., Zhang, R., Gottardi, C. J. and Caplan, M. J. (1993) Functional properties of an H,K-ATPase/Na,K-ATPase chimera. *J. Biol. Chem.* **268**, 10654–10658
- 145 Lyu, R. M. and Farley, R. A. (1997) Amino acids Val115–Ile126 of rat gastric H<sup>+</sup>-K<sup>+</sup>-ATPase confer high affinity for Sch-28080 to Na<sup>+</sup>-K<sup>+</sup>-ATPase. *Am. J. Physiol.* **272**, C1717–C1725
- 146 Asano, S., Matsuda, S., Hoshina, S., Sakamoto, S. and Takeguchi, N. (1999) A chimeric gastric H,K-ATPase inhibitable with both ouabain and SCH 28080. *J. Biol. Chem.* **274**, 6848–6854
- 147 Koenderink, J. B., Hermsen, H. P. H., Swarts, H. G. P., Willems, P. H. G. M. and De Pont, J. J. H. M. (2000) High-affinity ouabain binding by a chimeric gastric H<sup>+</sup>,K<sup>+</sup>-ATPase containing transmembrane hairpins M3–M4 and M5–M6 of the  $\alpha$ 1-subunit of rat Na<sup>+</sup>,K<sup>+</sup>-ATPase. *Proc. Natl. Acad. Sci. U.S.A.* **97**, 11209–11214
- 148 Farley, R. A., Schreiber, S., Wang, S.-G. and Scheiner-Bobis, G. (2001) A hybrid between Na<sup>+</sup>,K<sup>+</sup>-ATPase and H<sup>+</sup>,K<sup>+</sup>-ATPase is sensitive to palytoxin, ouabain, and SCH28080. *J. Biol. Chem.* **276**, 2608–2615
- 149 Ishii, T., Lemas, M. V. and Takeyasu, K. (1994) Na<sup>+</sup>-, ouabain-, Ca<sup>2+</sup>-, and thapsigargin-sensitive ATPase activity expressed in chimeras between the calcium and the sodium pump  $\alpha$  subunits. *Proc. Natl. Acad. Sci. U.S.A.* **91**, 6103–6107